NASA TECHNICAL NOTE

NASA TN D-7623

NASA TN D-7623

FURTHER ANALYSIS OF BROADBAND NOISE MEASUREMENTS FOR A ROTATING BLADE OPERATING WITH AND WITHOUT ITS SHED WAKE BLOWN DOWNSTREAM

by James Scheiman

Langley Research Center

Hampton, Va. 23665

NATIONAL AERONAUTICS AND SPACE ADMINISTRATION • WASHINGTON, D. C. • SEPTEMBER 1974

1. Report No.	2. Government Accession No.	3. Recipient's Catalog No.
NASA TN D-7623		

4. Title and Subtitle	5. Report Date
FURTHER ANALYSIS OF BROADBAND NOISE MEASUREMENTS FOR A ROTATING BLADE OPERATING WITH AND WITHOUT ITS SHED WAKE BLOWN DOWNSTREAM	September 1974
	6. Performing Organization Code
7. Author(s)	8. Performing Organization Report No.
James Scheiman	L-9349
	10. Work Unit No.
9. Performing Organization Name and Address	760-63-02-04
NASA Langley Research Center Hampton, Va. 23365	11. Contract or Grant No.
	13. Type of Report and Period Covered
12. Sponsoring Agency Name and Address	Technical Note
National Aeronautics and Space Administration Washington, D.C. 20546	14. Sponsoring Agency Code

15. Supplementary Notes

16. Abstract

An experimental investigation has been conducted to investigate the broadband noise generated by a rotating-blade system. Tests were made with circular and NACA 0012 rotor-blade sections. The blades were operated only with zero lift at each radial station. Tests were made both with zero axial velocity, so that the blades operated in their own turbulent wake, and with a small axial velocity imposed by the wind tunnel to blow the wake of one blade away before the passage of the next blade.

The rotor with cylindrical blades generally radiated more noise throughout the noise spectrum than did the rotor with airfoil blades. Blowing the blade wake away from the rotor with cylindrical blades did not have any appreciable effect on the amplitude frequency spectrum, and the predominant noise was broadband, either with tunnel wind on or off. For the rotor with airfoil blades, however, blowing the blade wake away changed the character of the noise spectrum completely in that broadband noise was eliminated or diminished to such an extent as to be indistinguishable. The broadband noise of the airfoil-bladed rotor with zero axial velocity is apparently caused by lift fluctuations due to velocity components of the turbulence normal to the plane of rotation.

With regard to the origin of broadband noise of rotors, nearly all of the evidence developed in the present investigation would indicate that it is caused by the shedding of Von Kármán type vortex streets. The amplitude of the broadband noise was found to scale as the sixth power of tip speed and the frequency varied directly as tip speed.

17. Key Words (Suggested by Author(s))	18. Distribution Statement
Broadband noise Rotating-blade noise Vortex noise	Unclassified – Unlimited STAR Category 01

19. Security Classif. (of this report)	20. Security Classif. (of this page)	21. No. of Pages	22. Price*
Unclassified	Unclassified	61	$3.75

*For sale by the National Technical Information Service, Springfield, Virginia 22151

FURTHER ANALYSIS OF BROADBAND NOISE MEASUREMENTS FOR A ROTATING BLADE OPERATING WITH AND WITHOUT ITS SHED WAKE BLOWN DOWNSTREAM

By James Scheiman
Langley Research Center

SUMMARY

An experimental investigation has been conducted in the Langley full-scale tunnel and outdoors to investigate the broadband noise generated by a rotating-blade system. Acoustic measurements were made at several different microphone positions, and the data were analyzed to obtain the 1/3-octave and narrow bandwidth frequency spectra. Tests were made with two markedly different airfoil blade sections, one a circular section (the "blade" was simply a piece of round tubing) and the other an NACA 0012 airfoil section having a thickness equal to the diameter of the circular section. The blades were operated only with zero lift at each radial station. Tests were made both with zero externally imposed axial velocity, so that the blades operated in their own turbulent shed wake, and with a small axial velocity imposed by the wind tunnel to blow the wake of one blade away before the passage of the next blade. For the wind-on tests, the rotor with airfoil-shaped rotor blades was given a small helical twist so that each blade element could operate at zero lift.

The rotor with cylindrical blades generally radiated more noise throughout the noise spectrum than did the rotor with airfoil blades. Blowing the blade wake away from the rotor with cylindrical blades did not have any appreciable effect on the amplitude frequency spectrum, and the predominant noise was broadband, either with tunnel wind on or off. For the rotor with airfoil blades, however, blowing the blade wake away changed the character of the noise spectrum completely in that broadband noise was eliminated, or diminished to such an extent as to be indistinguishable. Narrow-band analysis showed that actually the noise of the airfoil-bladed rotor operating in its own wake, which had appeared to be broadband in 1/3-octave-bandwidth analysis, was not classical broadband noise but was made up of noise peaks at many harmonics of blade passage frequency. This

pseudobroadband noise of the airfoil-bladed rotor with zero axial velocity is apparently caused by lift fluctuations due to velocity components of the turbulence normal to the plane of rotation.

With regard to the origin of broadband noise of rotors, nearly all of the evidence developed in the present investigation would indicate that it is caused by the shedding of Von Kármán type vortex streets. The amplitude of the broadband noise was found to scale as the sixth power of tip speed and the frequency varied directly as tip speed. This frequency scaling relation is consistent with the Strouhal relation; and a value of Strouhal number of 0.18, which is a representative value for vortex shedding frequency, was determined for the cyclindrical blades based on their thickness, tip speed, and the frequency for the peak amplitude of the broadband amplitude-frequency spectrum.

INTRODUCTION

One of the important, but poorly understood, types of noise generated by propellers and helicopter rotors is the so-called "vortex noise." The origin of this noise, which is characterized by being broadband, is controversial. Broadband noise consists of rotor noise that does not radiate at multiples of rotor rotational speed. Some believe that broadband noise originates from the shedding of Von Kármán type vortex streets behind an airfoil. The vortex shedding frequency, which is related to the Strouhal number N_{Str}, can be defined for a given relative airfoil velocity. The relative velocity varies along the radius of the rotating blade, and, therefore, there is a multitude of shedding frequencies, thus creating a broadband noise. Others believe that the broadband noise originates from changes in incidence caused by random turbulence ahead of the blade section. Since this turbulence is random, it will create a random pressure or lift fluctuation on the blade and the noise will be radiated as broadband noise. Either, or both, of these suggestions as to the source of broadband noise seems plausible. A shortage of experimental information on broadband noise has been a major impediment to defining the origin of this type of noise.

Generally, rotational and blade-slap noise (when present) are the dominant rotating-blade noise sources. Considerable effort is being directed toward the reduction of these two dominant noise sources. Methods are being studied and being applied to helicopter

operation to avoid blade-slap noise. Also, by reducing the blade rotational tip speed the rotational noise can be greatly reduced. With the reduction of these two noise sources, the remaining source, broadband noise, could become the dominant source. Further, for some rotating-blade systems, the broadband noise represents a substantial portion of the total noise heard by the human ear.

Many previous propeller noise experiments were conducted in still air (refs. 1 to 4). In such cases the blade can be operating in a turbulent wake of the preceding blade with the possibility of random fluctuating lift loads causing rotational noise. One technique for avoiding this problem is to operate a rotor with helically twisted blades in an axial velocity so that the blades are at zero lift all along their span. A helically twisted blade is defined as a blade with a spanwise blade-section pitch that is inversely proportional to the rotor radius. In this case the shed wake of each blade is carried away downstream before the passage of the next blade.

In the present investigation, experiments were conducted with the blade operating in its own shed wake and with the blade wake blown away. For both operating conditions, the blades were tested with zero lift force throughout their span. These tests were conducted at fairly large scale, with rotors of 3.05-m diameter. The Langley full-scale tunnel was used to provide a controlled axial velocity. The twisted blades operating with axial velocity were intended to produce noise due to vortex shedding; and the tests with untwisted blades operating with zero axial velocity would provide an opportunity to evaluate the effect of turbulence from the shed wake of the previous blade, namely shed-wake turbulence.

In addition to the foregoing basic program, numerous additional effects were investigated. For example, blade-tip shapes were changed and spoilers were added to the basic blade to increase its wake turbulence and drag. Effects of airfoil shape were investigated by testing a blade with a circular cross section having a radius and thickness equal to that of the airfoil section. Noise directivity was also determined.

The preliminary results of this program were published in reference 5. The data in reference 5 were based on a 1/3 octave and on overall noise measurements only. The data herein present a more detailed look at the results, and a narrow-band analysis of the noise data is provided.

SYMBOLS

D	rotor diameter, m
d	blade-section thickness, m
f	frequency, Hz
N_o	nominal rotor rotational speed, rpm
N_{Str}	Strouhal number, fd/U
r_H	hall radius, m
U	blade-section velocity, m/sec
V	axial velocity, m/sec
V_t	rotational blade tip speed, m/sec
x, y, z	coordinates of the microphone locations (see table II), m

APPARATUS AND TESTS

The test program was conducted in the 9- by 18-m Langley full-scale tunnel and outdoors. Outdoor tests were conducted to provide a base for evaluation of the reverberation effects. This section of the report describes the rotor model, the test setup, the data-acquisition system, and the data-reduction procedures.

Rotor Models

A two-bladed rotor system was used for this investigation. The blades were 3.05 m in diameter with a thickness of 5.08 cm. Two differently shaped airfoil sections were

used, a circular section and an NACA 0012 airfoil. The rotors are referred to herein as having cylindrical blades or airfoil blades. The rotor with the circular cross section was tested with various blade-tip shapes as shown in figure 1. The other two rotor models tested had NACA 0012 airfoil sections, one rotor having untwisted blades and the other having blades with a helical twist. The blade chord was approximately 42.4 cm. The airfoil section extended from the 0.305-m radius station to the blade tip. Photographs of the twisted and untwisted blades are shown in figures 2(a) and 2(b), respectively.

The NACA 0012 blades were tested with two different blade-tip shapes. One of the tips was a squared-off end and the other was a body of revolution with a radius equal to one-half the blade thickness at the chord station. Table I describes the various blade configurations and gives their configuration numbers.

An attempt was made to evaluate vortex-noise variations with airfoil-shape changes by fastening spoilers to the blade surface. Figure 3(a) indicates the location of the spoilers on the blade. For some other tests, No. 14 grit was applied to the leading edge of some of the configurations, as shown in figure 3. For additional details about the rotor model, reference 5 should be consulted.

Test Setup

The rotor was driven by a variable-frequency 746-kW electric motor that provided sufficient torque and a rotational-speed control of about ± 3 rpm. A photograph of the model setup in the wind tunnel is shown in figure 4. The rotor rotational axis was in the center of the tunnel and was approximately 3.96 m above the groundboard. The microphone locations for the wind-tunnel tests (indoors) are given in table II. A photograph of the model test setup for the outdoor tests is shown in figure 5. The rotor axis was alined parallel to and approximately 2.44 m above the ground level. The microphone locations for the outdoor tests are given in table II. These outdoor tests were conducted at a near-zero wind condition only (wind speeds that were judged to be less than about 2 cm/sec).

During the tests, wind screens (see fig. 6) were employed on all microphones except for microphone number 2, which was mounted in the groundboard in the indoor tests. These screens were employed to minimize the wind-noise effect on the microphones, and they have been shown to have no appreciable effect on the noise measurements below a frequency of about 15 000 Hz.

Data Acquisition

The noise-measurement equipment used for these tests was a commercially available system, and certain components can be seen in the photographs of figure 6. The microphones were a piezoelectric ceramic type having a 2.54-cm-diameter active diaphragm and a frequency response that was flat to within $\pm 1\frac{1}{2}$ dB over the frequency range from 20 to 12 000 Hz. An FM magnetic tape recorder was used to record the microphone outputs for these tests. All measurements were made in accordance with the recommendations of reference 6. The entire sound-measurement system was calibrated immediately before and after the acoustical measurements by means of discrete-frequency calibrators. The acoustical measurements were accepted only when the recorded pre- and post-calibration amplitude was within about 1/4 dB. In addition, the acoustical measurements were accepted only when the recorder voltages for each microphone were between peak-to-peak root-mean-square values of 1.0 and 2.8 volts.

Data Reduction

The data obtained from these tests were reduced by analog and by digital methods. The analog method was used to cross-check data as they were obtained. In order to obtain the detailed 1/3-octave-band information, digital computational methods were used. The data from the original analog tapes were played into a 1/3-octave-band parallel filter set. The output of the filter set was digitized and was then sampled every 1/2 second. Thus, at each 1/2-second interval, a complete 1/3-octave-band listing was obtained. Samples were taken over a 30-second interval and the results were averaged. The corresponding overall level was then computed by combining the averaged 1/3-octave-band amplitudes. It should be noted that the lowest 1/3-octave band (50 Hz) does not include the fundamental blade-passage frequency.

In addition to the 1/3-octave-band information, some limited narrow-band analysis was also performed. Analog data were digitized and formulated for input to a digital-computer program which employed Fast Fourier Transform techniques to do spectral analysis. Details of the program and the concomitant theory may be found in reference 7. The resultant spectra cover a range from 0 to 2000 Hz with a 4-Hz resolution.

RESULTS AND DISCUSSION

In general, the data are presented and discussed in the following order, each item generally being necessary for understanding of the succeeding items:

(1) Considerations such as test-chamber reverberation effects and effects of microphone position which influence the quality and interpretation of the noise measurements

(2) Effects of test variables such as rotor rotational speed and operation of the rotor in its own turbulent shed wake or in "clean air" with the wake blown away

(3) Effects of the configuration variables: blade airfoil cross section and tip shape

(4) Analysis of the data in terms of possible mechanisms of the noise generation, and the relation of the present data to other experiments or analyses

Considerations Regarding the Noise Measurements

Reverberation effects.- Before any noise test measurements inside a closed chamber are analyzed, the reverberation effects of the chamber must be evaluated. In the present program two methods were utilized. First, identical tests were conducted in the test chamber and outdoors, and the results were compared. These tests were conducted in as near zero-wind conditions as possible. The second method was to compute the "hall radius" from the known room characteristics (see ref. 8) and the measured model directivity from the outdoor tests. The hall radius is defined as the distance from the noise source where the sound pressure from the source is equal to the sound pressure from the reverberant field. The reverberation effects with tunnel speed were not evaluated; however, the tunnel-speed effect is expected to be small because the maximum test speed was only 6.1 m/sec.

A comparison of the indoor and outdoor measurements for a 1/3-octave-band analysis of the data is presented in reference 5. A comparison of the indoor and outdoor measurements for a narrow-band (4-cycle bandwidth) analysis is presented in figures 7 and 8. These two figures are for microphones alined with the rotor rotational axis and at a distance of 2 and 5.5 rotor diameters for figures 7 and 8, respectively. Figures 7(a) and 8(a) are for the rotor with cylindrical blades and figures 7(b) and 8(b) are for the rotor with the airfoil blades. As seen from the figures, the amplitude differences between the indoor and outdoor results seem to be quite uniform over the frequency range. Therefore,

it is concluded that the reverberation effects of the indoor tests will not greatly affect the amplitude frequency spectrum for frequencies between 0 and 2000 Hz.

The second method of reverberation evaluation was based on use of an estimated hall radius. The hall radius in reference 8 is for an omnidirectional source; therefore, the hall radius for the present models will be different because of the different directivity. The procedure used to estimate the hall radius for the present models is as follows.

It was assumed that the outdoor measurements were free-field measurements. This would seem to be a valid assumption since there were no solid objects within about 19 m of the test model, and the ground reflections from the grassy surface were small; also, this surface was fairly uniform within the microphone distances. From the microphones surrounding the outdoor test model, the total radiated power for each octave band was determined. The average power was determined and hence the directivity factor. The hall radius for each octave band was then computed from equation (9) of reference 8.

The results of these calculations are presented in figures 9 and 10. Since the radiation pattern is symmetrical about the rotational axis and since microphones were placed in a semicircle around the model, only a semicircle of the calculated hall radius is presented. Figure 9 is for the rotor with cylindrical blades and figure 10 is for the rotor with airfoil blades. The frequencies chosen for this analysis were those expected, from reference 8, to give the smallest hall-radius values. In other words, for frequencies below 125 Hz or above 2000 Hz, the hall radii are expected to be larger than those presented. This is because of the variation in reverberation times. The hall radii in these figures have been nondimensionalized by dividing by the rotor diameter D. The nondimensionalized hall radii presented in figures 9 and 10 are for variations in azimuth angles, variations in rotor rotational speed, and variations in the 1/3-octave-band-center frequencies. The 0° azimuth line is coincident with the rotor rotational axis (using right-hand rule). Figures 9 and 10 indicate that the hall radius in the 90° azimuth position (in the plane of rotation) is relatively small compared to that for the other positions. This characteristic is caused by the directivity factor or the relatively small amount of sound energy radiated in the plane of the rotor as compared to the sound radiated along the axis of the rotor. Also, the hall radius is slightly more uniform with azimuth angle for the rotor with cylindrical blades (fig. 9) than for the rotor with airfoil blades (fig. 10). This characteristic is due to the differences in the sound radiation of the two rotors.

At 1 hall-radius distance the measured noise will be 3 dB above that of the free-field noise source. At 1/2 and 2 hall-radii distances the measured noise will ideally be 1 and 7 dB above that of the noise source, respectively. From the results in figures 9 and 10, 1 hall radius is about equal to or greater than 2 rotor diameters for azimuth angles from 0° to 45° and from 135° to 180°. Therefore, keeping the measuring microphones within these azimuth angles and at a distance of 2 rotor diameters, or less, will insure that the reverberant field effect is 3 dB or less. Because of the relatively small hall-radius value in the plane of the rotor (90° azimuth position), only the ground-reflection microphone (microphone position 2) was placed in this position for the indoor tests. It is concluded that (1) the reverberation effects for these tests are relatively small, and (2) the computed hall radius can be used to evaluate the reverberation effects.

The near-field effect is another aspect of the microphone location problem and is defined by the lowest acoustic frequency of interest. The frequency corresponding to a wavelength equal to a 2-rotor-diameter distance is about 50 Hz. Therefore, a lower frequency boundary of 50 Hz corresponds to near-field limits for a microphone located at a 2-rotor-diameter distance. (This corresponds to the lowest frequency band presented in ref. 5.) Thus, choosing to locate the microphones at a 2-diameter distance was a compromise between minimizing the reverberant field and staying in the far field.

The difference between the indoor and outdoor results in figure 7 for the microphone at a 2-diameter distance is between 2 and 5 dB. This difference agrees reasonably well with the 1 to 3 dB expected from the hall-radius calculation. The difference between the indoor and outdoor results for the microphone at a 5.5-diameter distance is between 5 and 10 dB (fig. 8). This distance corresponds to 2.75 hall radii, or less (for some frequencies), which results in a reverberation effect of 7 to 11 dB being expected. Again the estimated and measured reverberation effects agree reasonably well.

Repeatability of data.- Figure 11 is a plot of the 1/3-octave-band sound-pressure level against the centerband frequency for the same test performed on two different days. The plot is for two microphone positions and two different rotational speeds for the rotor with cylindrical blades in outdoor tests. The figure shows that the data are repeatable within 1 dB. Limited additional comparisons were made with the same conclusions, namely, repeatability within about 1 dB.

Ground reflectivity.- Figure 12 shows the 1/3-octave-band level differences between a microphone mounted in the ground (microphone position 11), where it is not exposed to

reflections, and a microphone mounted on a stand 2.44 m above the ground (microphone position 10). Figure 12 shows that, for the frequencies and microphone heights used herein, the ground-reflectivity effects present are reasonably small.

Effects of microphone position.- There are very definite effects of microphone position on the characteristics of the noise measured from a rotor which should be recognized in analysis of the data. Ideally, along the rotational axis no rotational noise should be measured. There is no Doppler shift; and, therefore, there is a one-to-one relationship between input modes and output harmonics. Further microphone measurements can be directly related to fluctuating forces on the rotor disk. Thus, the levels of these forces can be inferred from the on-axis acoustics.

Reference 9 indicates that, in the ideal case, broadband noise of a rotating-blade system will radiate as a dipole with the maximum amplitude along the rotational axis and with zero amplitude in the plane of rotation. Also, rotational noise will radiate as a dipole with the maximum amplitude in the plane of rotation and with zero amplitude along the axis of rotation. The noise measurements of the present investigation were made with microphones located along the axis of rotation, in the plane of rotation, and at a 45° azimuth station between the axis and plane of rotation. Presumably, the noise measured at the 45° station would possess characteristics of both broadband and rotational noise.

The data of the present investigation are generally consistent with these patterns. For example, the narrow-band amplitude-frequency spectra of figure 13 for the rotor with cylindrical blades and the corresponding data of figure 14 for the rotor with airfoil blades show a predominance of broadband noise when the microphone was located on the axis of rotation. When the microphone was located in the plane of rotation the predominant noise was at low frequencies at low harmonics of blade-passage frequency. The data of figures 13 and 14 are not the same as the ideal case, however, because there was a substantial sound-pressure peak at the first harmonic of blade-passage frequency recorded by the microphone along the axis of rotation, and there was some evidence of broadband noise at a low amplitude when the microphone was in the plane of rotation. The corresponding 1/3-octave-band spectra of figure 15 show evidence of the characteristics brought out by figures 13 and 14. Similar 1/3-octave-band spectra when the microphone was located at 45° to the axis of rotation are shown in figure 16. These data, as might be expected, show evidence of both broadband noise and rotational noise at the low frequencies which correspond to the low harmonics of blade-passage frequency.

Effect of Operating Blades in Shed-Wake Turbulence

Tests were made at zero wind speed with the blades operating in their own shed wake and with an axial wind to blow the wake of one blade away before the passage of the next blade. For both operating conditions, each radial blade section was operating at 0° angle of attack. It should be recalled that, in order to permit operation of the airfoil blades at 0° angle of attack with wind on, one set of blades was fabricated with a helical twist, and the wind velocity was matched to the rotational speed so that the advance ratio exactly matched the helical twist of the blades. The results of this experiment were expected to have two applications: the first was to determine the effects of turbulence, such as that generated by passage of the preceding blades at zero wind speed, on the noise of the rotor, and the second was to provide some understanding of the significance of, and interpretation to be placed on, the results of experiments conducted in the past to evaluate broadband noise by operating a rotor at zero lift with zero axial air velocity (for example, ref. 2).

Figure 17 shows the 1/3-octave amplitude-frequency spectra of the rotor with cylindrical blades operating at various axial velocities. These data are for a microphone located along the axis of rotation and for a microphone located at 45° to the axis of rotation. The data show that for either microphone position there was similar broadband noise for the cylindrical blades whether the rotor operates in its own shed wake or whether the wake is blown away. This fact will be compared later to the case for the rotor with airfoil blades; but, first, two observations should be made with regard to the data of figure 17 for the cylindrical blades. One point is that increasing the axial velocity increased the total sound-pressure level slightly, and the second point is that the increase occurred almost entirely on the low-frequency side of the peak of the broadband noise.

It might seem reasonable that increasing axial velocity would increase the noise because it would increase the dynamic pressure on the rotating-blade sections. If one examines the situation quantitatively, however, it does not seem that the magnitude of such an increase in blade dynamic pressure is consistent with the magnitude of the increase in sound-pressure level. Broadband noise varies approximately as the sixth power of airspeed; then, almost all the noise would seem to be generated near the tip. However, the increase in velocity at the tip is so small as to be insignificant. For example, for the case of a rotational speed of 850 rpm, the airspeed at the tip increases from 135.6 m/sec at $V = 0$ m/sec to 135.7 m/sec at $V = 6.10$ m/sec. Such an increase of less than 0.1 percent in tip speed would not seem to account for the observed increase in noise.

Figure 18 presents a comparison of the amplitude-frequency spectra for the airfoil blades with and without axial air velocity. These data show that the broadband noise, which appears to be present when the rotor is operating in its own shed wake (zero axial velocity), is not present when the shed wake is blown away, and that the introduction of axial velocity decreases the overall sound-pressure level between 5 and 8 dB. When the wake is blown away, the spectrum levels for the frequencies between 100 and 2000 Hz are very near the wind-tunnel ambient level. The data also show that for the case when the shed wake is blown away, the amplitude level increases for frequencies of about 8000 Hz. The reason for this peak is not understood. It might be conjectured that the peak is actually the broadband noise for these blades, but there is no support for such a hypothesis.

Figure 19 presents data for a wide range of rotational speeds to show that wind-on data of figure 18 are not unique to the particular test conditions. These data show that the general character of the frequency spectrum is the same for all of the rotational speeds and that the noise level increases with increasing rotor rotational speed.

Broadband noise which is present and centered about a frequency of approximately 400 Hz when the rotor with airfoil blades was operated in its own shed wake is not present when the wake is blown away by an axial velocity. The data of figure 19 imply that the broadband noise was caused by shed-wake turbulence on the following blade and not by vortex shedding. It is hypothesized, as will be explained in detail later, that this broadband noise, when the airfoil blades operate in their own shed wake, is caused by fluctuating lift forces resulting from fluctuations of velocity components of the turbulence normal to the plane of rotation. When regarding the question as to whether differences in the models might have biased the data, it might be observed that the blade has a small amount of twist which would in turn tilt the dipole radiation axis along the blade radius; however, it is expected that this small amount of twist would tend to broaden the directivity pattern rather than eliminate the broadband noise as was the case herein.

Figures 20 and 21 present narrow-band spectra which show additional characteristics of the noise produced by the rotors with cylindrical and airfoil blades with and without the shed wake blown away by axial air velocity. Figure 20 is plotted to show directly the effects of forward speed, and figure 21 is plotted to show directly the effects of blade section. The data show, as did figure 17, that the cylindrical blades produce broadband noise with or without the wake blown away. For the airfoil blades, there is no broadband noise with wind on. In addition, what appeared to be broadband noise with wind off (in the 1/3-octave-band analysis) is to a large extent noise at many harmonics of blade-passage

frequency. The data also show that for both blade sections with wind on, there were pronounced peaks of noise at low harmonics of blade-passage frequency, but that the amplitude of these harmonics diminished rapidly with harmonic number.

The effects of blowing the wake away for the case of the airfoil blades might be explained as follows: As suggested previously, velocity components normal to the plane of rotation due to the shed wake of the preceding blade, or blades, would cause a variation in lift, or pressure, on the airfoil blades as a result of their lift-curve slope. These fluctuating lift forces would cause noise. Such noise would not be present when the wake was blown away and would not be present for the cylindrical blades which would have no lift-curve slope. It should be noted that the data of figures 20 and 21 were obtained with a microphone position on the rotational axis and 2 diameters from the plane of rotation. When the microphone is on the rotational axis, there is a direct relation between the pressure fluctuations on the blade and at the microphone. Therefore, fluctuating pressures reflect what is happening on the blade itself.

The fact that the noise due to the wake of the previous blades is periodic at harmonics of the blade-passage frequency might be explained as follows: Any flow velocity disturbance perpendicular to the rotor rotational plane (for example, shed vortex streets) will create an angle-of-attack change on the airfoil. A blade with a lift-curve slope will respond with a lift pulse and produce an induced velocity opposite to the direction of the initial disturbance. The following blade will now see two disturbances in opposite directions, one being the initial disturbance and the other being the induced disturbance. This process will continue until the entire blade revolution contains equally spaced disturbances. The periodic nature of the spectrum for the case of the rotor operating in its own shed wake shows that there is a fluctuating harmonic lift. This fact implies that the induced velocity variations must have the proper phase relationship for both blades to produce the same fluctuations at the same time. Further, the fluctuations must be evenly spaced around the azimuth and repetitive with each revolution (nonrandom).

In summary, the effects of turbulence are seen to be as follows:

(1) The rotor with cylindrical blades produced broadband noise, and this noise was essentially the same whether the blades were operating in their own turbulent shed wake or whether they were operating in "clean air" with the shed wake blown away.

(2) The character of the noise for the rotors with the airfoil blades was completely different; however, the characteristics of their difference depends on whether the blades operated in their own wake or in "clean air."

(3) When the airfoil blades were operated with their shed wake blown away, they did not create broadband noise and the noise was relatively low.

(4) When the airfoil blades were operated in the turbulence of their own shed wake they created a pseudobroadband noise which actually consisted of noise at many harmonics of blade-passage frequency, and the level of the noise was much higher than when the blades were operated in "clean air."

Effect of Rotor Rotational Speed

Figure 15 presents 1/3-octave-band frequency-amplitude spectra for both cylindrical and airfoil blades for various rotor rotational speeds. These data are from outdoor tests with zero axial velocity; and the microphones were located on the axis of rotation and in the plane of rotation. As pointed out in the discussion of the effects of microphone position, broadband noise is clearly defined for the case of the microphone on the axis of rotation for either the cylindrical blades or the airfoil blades. The peak of this broadband noise increases in both frequency and amplitude with increase in rotor rotational speed. For the case of the microphone located in the plane of rotation, there was no clearly defined broadband noise, as explained in the discussion of the effect of microphone position. For the case of the cylindrical blades, however, there did seem to be some broadband noise present, and the frequency and amplitude of the peak of this noise did seem to increase with increasing rotor rotational speed.

Figure 16 presents data from indoor tests which show noise spectra for a microphone located at 45° to the axis of rotation. These data show broadband noise with the peaks increasing in both frequency and amplitude with increase in rotor rotational speed.

Figures 13 and 14 present narrow-band (4-Hz bandwidth) frequency-amplitude spectra. These figures present more detailed information on the same data presented in figure 15 for a 1/3-octave-bandwidth spectra. The data show that the low frequency noise at low multiples of blade-passage frequency increase in amplitude and frequency with increase in rotational speed.

The foregoing observations about the effects of rotor rotational speed are all qualitative. In order to determine whether the data actually scaled according to conventional

scaling laws, the data of figure 15 are scaled in figures 22 and 23. The amplitude was scaled as the sixth power of the rotational speed. The frequencies were scaled directly as rotational speed since many aerodynamic phenomena are functions of nondimensional distance (for example, chord lengths) traveled. Such scaling is consistent with the Strouhal concept. Actually, on the plots, the center frequency of the 1/3-octave band has been divided by the tip rotational speed.

The data of figures 22 and 23 show that when broadband noise predominated (when the microphone was on the axis of rotation), the data collapsed fairly well into one curve, and, therefore, it scaled according to the scaling factors used. For the case of the microphone in the plane of rotation, however, the data did not scale according to the assumed parameters. In fact, since the data for the lower rotational speeds are generally above that for higher rotational speeds, it would seem that noise at the harmonics of blade-passage frequency scale in amplitude by some factor less than the sixth power of speed.

An additional attempt at applying the foregoing scaling relations was made for the case of data taken in the wind tunnel with the airfoil blades, both with and without the wake blown away. The results of this analysis are presented in figures 24 and 25 and are similar to those of figures 22 and 23. Specifically, when the predominant noise was broadband, as was the case with zero axial velocity, and the microphone was located on the axis of rotation (fig. 25(a)), the data scaled well; and when there was no broadband noise, as was the case when the wake was blown away (fig. 24), the data did not scale well.

Effect of Airfoil Cross Section and Tip Shape

Figure 26, which is a replot of data from figures 17 and 19, presents a direct comparison of the effect of airfoil shape, or blade from drag, on noise. These data are for the case in which the shed wake was blown away by an axial air velocity so that they show only the effect of blade form drag and not the effect of self-induced incident turbulence. All of the other data presented to show the effect of airfoil cross section were obtained at zero axial velocity where it has been shown that the noise of the airfoil blades is strongly influenced by the effect of incident turbulence from the preceding blades.

The data of figure 26 show a very large change in both the amplitude and spectrum of the noise with change from cylindrical to airfoil blades. The airfoil blades reduced the total noise about 15 dB and did not have the broadband noise which was characteristic of

the cylindrical blades. The 15-dB difference in noise level is consistent with reference 4 which indicates that the radiated noise power from a rotating blade is proportional to the square of the section drag coefficient. Since sound pressure is proportional to the square root of sound power, the sound pressure should be directly proportional to section drag coefficient. On this basis the approximately 6-to-1 ratio of drag coefficients of the circular and airfoil blade cross sections would be expected to result in the observed 15-dB increase in total sound-pressure level. In view of the greatly different character (spectra) of the noise from the two different blades, however, one cannot be sure whether it is proper to so relate the data of figures 17 and 19 to the results of a markedly different type of experiment in reference 4 wherein the tests were run at zero axial air velocity.

Since it has been indicated that the broadband noise of airfoil blades operating in their own shed wake is probably caused by lift fluctuations due to turbulence and their lift-curve slope, comparisons of the cylindrical and airfoil blades at zero axial velocity cannot be considered to show the effects of form drag. However, they might be of interest in terms of their relation to other investigations that have been run under these conditions. Figure 27 shows amplitude-frequency spectra for such a comparison and shows that the cylindrical blades create sound-pressure levels that are about 5 to 15 dB higher over the frequency range.

Tests with spoilers in the present investigation, which were run only at zero axial velocity, also show the effects of the spoilers on the noise of the airfoil blades. Grit was added to the airfoil before the spoilers were added; therefore, the effects of adding the grit must be evaluated before the effects of adding the spoilers can be determined. Figure 28 presents the 1/3-octave amplitude-frequency spectra for the rotor with airfoil blades with and without leading-edge grit added. (See fig. 3 for grit location.) The data are for various rotor rotational speeds and for microphones on the rotor rotational axis (fig. 28(a)) and in the rotor rotational plane (fig. 28(b)). These data show that the noise level and frequency distribution were not affected by the grit.

Adding spoilers to the airfoil would be expected to increase the section drag, to reduce the lift-curve slope, and to increase the shed-wake turbulence. The spoilers were added to the upper and lower surfaces simultaneously in order to avoid any blade torsion loads. Figure 29 presents 1/3-octave frequency-amplitude spectra showing the effect of the spoilers for variations in rotor rotational speed and microphone position. Figure 29(a), for the case of a microphone alined with the rotational axis, indicates that adding the

rearward spoilers increased the overall sound-pressure level about 6 to 8 dB. Adding the second set of spoilers resulted in an increase from 0 to 2 dB.

Recalling the previously described important influence of wake turbulence on the noise radiation, the change in noise level caused by the spoilers might be attributed to the change in wake turbulence due to the spoilers rather than to increases in the section drag due to the spoilers. This possibility seems especially likely since wind-on tests have shown no significant broadband noise such as that shown in figure 29(a) when the shed turbulent wake was blown away. It also seems especially likely since blade drag would be expected to radiate as rotor torque which ideally radiates as a dipole with the maximum amplitude in the plane of rotation and a minimum amplitude along the axis of rotation where the greatest effects of the spoilers were noted.

Figure 29(a) also shows that the frequency at the peak amplitude of the broadband noise has been decreased by adding the spoilers. This change in frequency would be expected if the Strouhal number N_{Str} is a constant because increasing the shed-wake thickness with spoilers should result in a decreased frequency.

Figure 29(b), for the microphone in the blade rotational plane, does not indicate any clear trends regarding the effect of adding the spoilers except that both the total noise and the sound-pressure level at all frequencies are greater when spoilers are added. This lack of a clear-cut trend for noise measured by the microphone in the plane of rotation was also shown in previous figures. (For example, see fig. 23.)

Figure 30 is a plot of the narrow-band noise spectra for the rotor with airfoil blades with and without spoilers. These data show that, for the case of the microphone alined with the rotational axis, adding the spoilers increases the amplitude of the broadband noise and decreases the frequency of the peak amplitude of the broadband noise, which is the same result as that shown by the 1/3-octave-band data of figure 29(a). Also shown in figure 30(b) is the fact that the amplitude and number of harmonics of blade-passage frequency present has been decreased by adding the spoilers. It should be recalled that these data are for the rotor operating at zero axial velocity (in its own shed wake) at a 0° mean blade angle of attack. Further, the existence of fluctuating pressures at harmonics of blade-passage frequency are normally defined as rotational noise and this noise is associated with a thrusting rotor. Therefore, it is supposed herein that the rotor is subjected to shed incident turbulence and lift fluctuations and that the spoilers decrease the blade-section lift-curve slope and, therefore, decrease the amplitude of the lift fluctuations caused by this turbulence.

For the case of the microphone in the rotor-blade rotational plane, figure 30(b) shows these same trends. Namely, adding the spoilers tends to decrease the amplitude and the number of harmonics present. Adding the spoilers does not seem to increase the amplitude of the sound-pressure level at the low harmonics of blade-passage frequency, but it does increase the amplitude of the broadband, or pseudobroadband, noise centered around frequencies of 400 Hz to 500 Hz, which is not the predominant noise source.

It is concluded from the wind-on tests of the dissimilar cylindrical and airfoil blades that the amplitude of the broadband noise may be proportional to the section drag of the rotating blade. However, because of the importance of wake turbulence with the associated harmonic lift noise, no definite conclusions can be drawn from the tests at zero axial velocity for similar airfoil blades with and without spoilers.

Effect of Blade-Tip Shape

Numerous blade-tip shapes have been tested in the past to determine their effect on rotor noise. Some of these tests have been successful in reducing the rotating-blade noise level. The reasons for the successes and failures are not completely understood. This lack of understanding is believed to be partly caused by the presence and interactions of all the different noise sources acting together. It was hoped that this problem might be clarified to some extent by determining the effect of blade-tip shape on the broadband noise alone. Four tip shapes were tested on the cylindrical blades (see fig. 1) and two tip shapes were tested for the rotor on the airfoil blades.

Figure 31 shows the effect of the different blade-tip shapes on the rotor with cylindrical blades for variations in rotor rotational speed, axial velocity, and microphone position on the 1/3-octave-band amplitude-frequency spectra. (Fig. 31(a) is for the case of a microphone alined with the rotor rotational axis and fig. 31(b) is for the case of a microphone at 45° to the rotor rotational axis.) All of these data show that, except for the frequencies between 1250 and 3150 Hz, the differences in amplitude are within the overall accuracy of measurement and data reduction. (See data repeatability in fig. 11.) The amplitude deviation between frequencies of 1250 and 3150 Hz occurs only on the model with the opened blade tip, and the depth of the open end corresponds to the expected organ-pipe frequency that was observed.

Figure 32 presents similar 1/3-octave-band amplitude-frequency spectra for the rotor with airfoil blades with the two different tip shapes tested. Variations in microphone

position and axial velocity are presented. Microphone position 5 is alined with the rotor rotational axis, and microphone positions 1 and 3 are at 135° and 45° to the rotor rotational axis. It should be recalled that one blade tip had a squared-off end (models 10 and 20) and the other blade tip was a body-of-revolution (models 11 and 21). From figure 32 it is seen that there is no appreciable change in the overall amplitude level. However, there are some amplitude variations in the amplitude-frequency spectrum, especially for the case with the rotor operating with axial velocity, in which case the rotor with the squared-off tip made more noise at very high frequencies than did the rotor with the body-of-revolution tip. The reasons for this variation with axial velocity are not understood. It is interesting to note that the spectrum in figure 32 for microphones 1 and 3 (at 45° ahead of and behind the rotor rotational plane) are similar, indicating that the directivity is symmetrical about the rotor rotational plane.

Figure 33 is a plot of the narrow-band analysis of the noise amplitude showing the effect of the tip-shape changes for the rotor with airfoil blades and the rotor with cylindrical blades. The agreement for the different tip shapes is quite good, especially where the numerous harmonics of blade-passage frequency are present. This is particularly interesting for the rotor with cylindrical blades (fig. 33(a)) since the blade tips tested had radical shape changes. (See fig. 1.)

From the foregoing data and analysis, it is concluded that for the tip shapes chosen there is very little effect of tip shape on the broadband noise radiation.

Discussion of Data

In the "Introduction" it was pointed out that there were two principal postulations as to the source of broadband rotor noise. One postulation was that it was caused by the blade lift fluctuations resulting from the shedding of Von Kármán type vortex streets behind the blades, and the other was that it was caused by turbulence ahead of the blades inducing random fluctuations of blade lift. This second possibility seemed particularly likely for the case of experiments wherein airfoil-shaped blades were run at zero lift (operating in their own shed-wake turbulence).

The present tests have shown the postulation with regard to the effect of shed incident turbulence to be true for blades with an airfoil cross section run in their own shed wake. This result is shown by figure 18 which shows broadband noise when the airfoil-bladed rotor was run in its own wake, and it shows that there was no such broadband noise

(or that the noise level was so low as to be indistinguishable) when the blades were run in "clean air" with the shed wake carried away by a small axial air velocity. Actually, it should be noted from the narrow-band frequency spectra of figures 20(b) and 21(b) that the noise that appears to be broadband in a 1/3-octave-band analysis for the case of the airfoil-bladed rotor run in its own shed wake is actually noise at many harmonics of the blade-passage frequency and not classical broadband noise.

On the other hand, the cylindrical blades created about the same broadband noise whether run in their own wake or run in "clean air," as shown in figure 17, at frequencies at and below that for the peak of the amplitude-frequency distribution. This result might be consistent with the postulation that broadband noise is caused by the vortex shedding. If it is presumed that vortex shedding is the cause of the broadband noise for the cylindrical blades, then it would seem that the shed vortices must be much stronger than for the airfoil blades.

It is interesting to note, as shown in figure 27, that the amplitude-frequency distribution of the broadband noise is the same for the cylindrical and airfoil blades when run in their own turbulent shed wake. The vortex shedding frequency for the two blades is the same according to the Strouhal relation and their similar blade thicknesses. This result seems to indicate that the vortex streets from the airfoil blades were still sufficiently well formed when the following blade encountered them to give alternate positive and negative changes in angle of attack at the vortex shedding frequency.

With regard to the relationship of the frequency of the broadband noise to Strouhal number and vortex-shedding frequency, if a Strouhal number N_{Str} is calculated from the blade thickness, tip speed, and the frequency of the peak of the broadband noise amplitude-frequency spectrum for the cylindrical blades, a value of 0.18 is obtained. This is a representative value of the Strouhal number for the shedding of vortices from an airfoil; and this relation would seem to indicate that vortex shedding might be the source of the broadband noise for the cylindrical blades. This statement must be limited to the blades with cylindrical cross section, because the airfoil blades did not produce any noticeable broadband noise when their wake was carried away by an axial velocity, perhaps because the vortices are weak as a result of the low drag of the airfoil section.

A few observations seem to be in order with regard to why the noise is broadband since it is generally presumed that an airfoil sheds vortices at a discrete frequency. It has been suggested that the broadband character might be the result of different vortex-shedding frequencies because of the different airspeed of the blade at different radial

stations. This explanation does not bear close inspection, however, since aerodynamic noise varies approximately as the sixth power of airspeed and almost all the noise would be expected to be generated very near the tip where the velocity is highest and where the shedding frequencies would occupy a very narrow band. A more appropriate explanation might be that two-dimensional airfoil tests such as those of reference 10 show that even a two-dimensional airfoil creates broadband noise. On this basis, even the outermost tip sections of the rotor alone would be expected to produce broadband noise. However, these observations do not provide an entirely satisfactory explanation: partly because the mechanism of the broadband noise of the fixed wings is not understood, and partly because the frequency from the tests of reference 10 is four times smaller than that of the present test.

The data of figures 13(b) and 14(b) for the cylindrical and airfoil blades, respectively, both show that the predominant in-plane noise was at the first two or three harmonics of blade-passage frequency, as would be expected for rotational noise; the data also seem to show, however, that there is some minor broadband noise which peaks at about 400 Hz, depending on the rotational speed. If broadband noise along the axis of rotation is caused by vortex shedding, presumably by the alternate plus and minus lift loads caused by the shedding of alternate vortices, then it might be presumed that this vortex shedding would cause a fluctuating drag load also, which might cause broadband noise to be measured in the plane of rotation. Such a hypothesis has been advanced previously, but the present data do not support the hypothesis because the frequency of the drag fluctuations would be twice that of the lift fluctuations; however, the present data do show the peak of this minor in-plane broadband noise to be at about the same frequency as that of the broadband noise measured along the axis of rotation.

CONCLUSIONS

An investigation was conducted in the Langley full-scale tunnel and outdoors to define further the characteristics of the broadband or so-called "vortex" noise generated by a rotating-blade system. The rotor blades were operated at 0° mean angle of attack throughout their span – both with and without axial velocity. The following conclusions are offered:

1. The tunnel reverberation effects were evaluated by two different methods and the comparison is reasonably good. The microphones for the main body of the investigation were kept within 1 "hall-radius" distance; therefore, the reverberation effects were 3 dB, or less.

2. When the rotor-blade wake was blown away with a small axial velocity so that blades operated in "clean air," the following results were found:

(a) The cylindrical blades created a great deal more noise than the airfoil blades.

(b) The noise for the cylindrical blades had a pronounced broadband character although there was a very high peak of sound pressure at the blade-passage frequency.

(c) There was no evidence of broadband noise for the airfoil blades.

(d) The noise for the airfoil blades was predominately at low harmonics of blade-passage frequency and diminished rapidly with harmonic number, being practically indistinguishable beyond the fourth harmonic.

3. When the blades were operated in their own wake turbulence with zero axial velocity, the following results were found:

(a) The noise for the cylindrical blades was little different than for the case of operation in "clean air."

(b) The noise for the airfoil blades increased markedly and took on a pseudo-broadband character.

(c) Narrow-band spectra showed this pseudobroadband noise to consist of sound-pressure peaks at many harmonics of blade-passage frequency, the peaks being clearly distinguishable to about the 30th harmonic.

(d) The pseuodbroadband noise for the airfoil blades operated in their own wake would seem to be caused by blade lift fluctuations resulting from the lift-curve slope of the blades together with the normal-to-the-plane velocity components of the incident turbulence.

4. Increasing rotor rotational speed resulted in the following:

(a) Increased frequency for the peak sound-pressure level for the broadband noise of the cylindrical blades, and an increase of the pseudobroadband noise of the airfoil blades operated in their own wake, the frequency varying directly as tip speed.

(b) Increased sound-pressure level for all conditions.

5. For the blade-tip shapes tested, there was no significant effect of tip shape on the frequency spectrum.

6. With regard to the postulation that broadband noise is caused by vortex shedding, the following observations were made:

(a) Other investigations have shown that broadband noise is created by an ordinary, nonrotating airfoil; thus, broadband noise could be created by a nonlifting rotor, even though almost all of the noise was caused by the outermost parts of the blade.

(b) A value of Strouhal number of about 0.18 was obtained based on blade thickness, tip speed, and frequency for the peak amplitude of the broadband noise of the cylindrical blades or the pseudobroadband noise of the airfoil blades. This value of Strouhal number is a representative value for a two-dimensional airfoil.

(c) The fact that the airfoil did not create any recognizable broadband noise when operated in "clean air," with the blade wake blown away, might simply indicate that the shed vortices were too weak because of the low drag of the section to induce significant lift pulsations.

Langley Research Center,
National Aeronautics and Space Administration,
Hampton, Va., May 29, 1974.

REFERENCES

1. Ernsthausen, W.: The Source of Propeller Noise. NACA TM 825, 1937.

2. Deming, A. F.: Noise From Propellers With Symmetrical Sections at Zero Blade Angle II. NACA TN 679, 1938.

3. Stowell, E. Z.; and Deming, A. F.: Vortex Noise From Rotating Cylindrical Rods. NACA TN 519, 1935.

4. Yudin, E. Y.: On the Vortex Sound From Rotating Rods. NACA TM 1136, 1947.

5. Scheiman, James; Hilton, David A.; and Shivers, James P.: Acoustical Measurements of the Vortex Noise for a Rotating Blade Operating With and Without Its Shed Wake Blown Downstream. NASA TN D-6364, 1971.

6. Anon.: Measurements of Aircraft Exterior Noise in the Field. ARP 796, Soc. Automot. Eng., Inc., June 15, 1965.

7. Brown, Thomas J.; Brown, Christine G.; and Hardin, Jay C.: Program for the Analysis of Time Series. NASA TM X-2988, 1974.

8. Vér, István L.; Malme, Charles I.; and Meyer, Eugene B.: Acoustical Evaluation of the NASA Langley Full-Scale Wind Tunnel. Rep. No. 2100 (Contract No. NAS1-9559), Bolt Beranek and Newman, Inc., Jan. 22, 1971. (Available as NASA CR-111868.)

9. Richards, E. J.; and Mead, D. J., eds.: Noise and Acoustic Fatigue in Aeronautics. John Wiley & Sons, Ltd., 1968.

10. Potter, R. C.: An Experiment To Examine the Effect of Porous Trailing Edges on the Sound Generated by Blades in an Airflow. NASA CR-66565, 1968.

TABLE I.- MODEL CONFIGURATION NUMBER AND DESCRIPTION

Configuration	Blade description	Blade-tip description
00	5.08-cm-diameter cylinder	Open end of pipe
01	5.08-cm-diameter cylinder	Squared tip
02	5.08-cm-diameter cylinder	5.08-cm-diameter hemisphere
03	Same as configuration 01 with No. 14 grit added to leading edge (see fig. 3(b))	Squared tip
04	5.08-cm-diameter cylinder	10.16-cm-diameter end plate
10	Untwisted NACA 0012 airfoil	Squared off
11	Untwisted NACA 0012 airfoil	Body of revolution
20	Twisted NACA 0012 airfoil	Squared off
21	Twisted NACA 0012 airfoil	Body of revolution
12	Same as configuration 10 with No. 14 grit added to leading edge (see fig. 3(a))	Squared off
13	Same as configuration 12 with rearward chord spoilers (see fig. 3(a))	Squared off
14	Same as configuration 13 with forward chord spoilers (see fig. 3(a))	Squared off

TABLE II.- MICROPHONE LOCATIONS

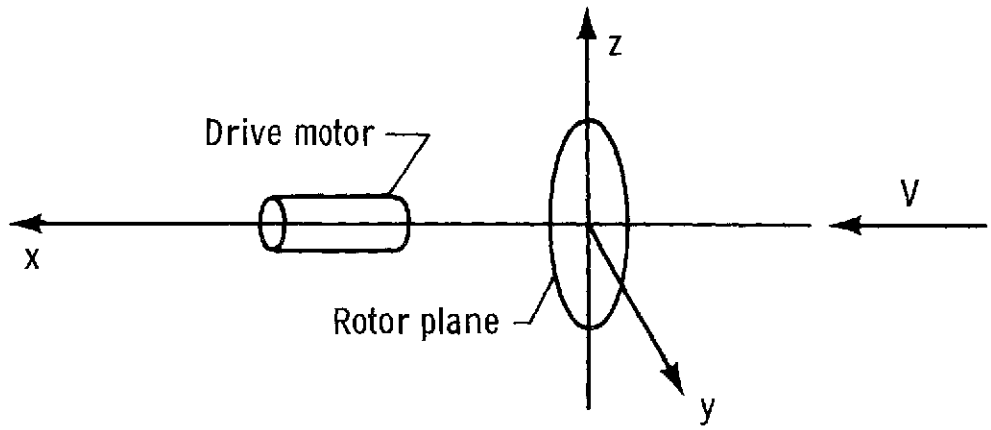

Microphone number	Actual locations			Nominal location	
	x, m	y, m	z, m	Distance from rotor center, in rotor diameters	Degrees from X-axis
Indoors in Langley full-scale tunnel					
1	-4.47	4.3	-0.61	2	135
2	0	-.10	-4.06	1.6	90
3	4.32	4.32	-.30	2	45
5	-6.1	0	.05	2	180^{o}
6	-16.84	0	-.20	5.5	180^{o}
Outdoors in free field					
7	-16.7	0	0	5.5	180^{o}
10	-5.84	0	0	2	180^{o}
11	-6.61	0	-2.44	2	180^{o}
15	.10	6.1	0	2	90

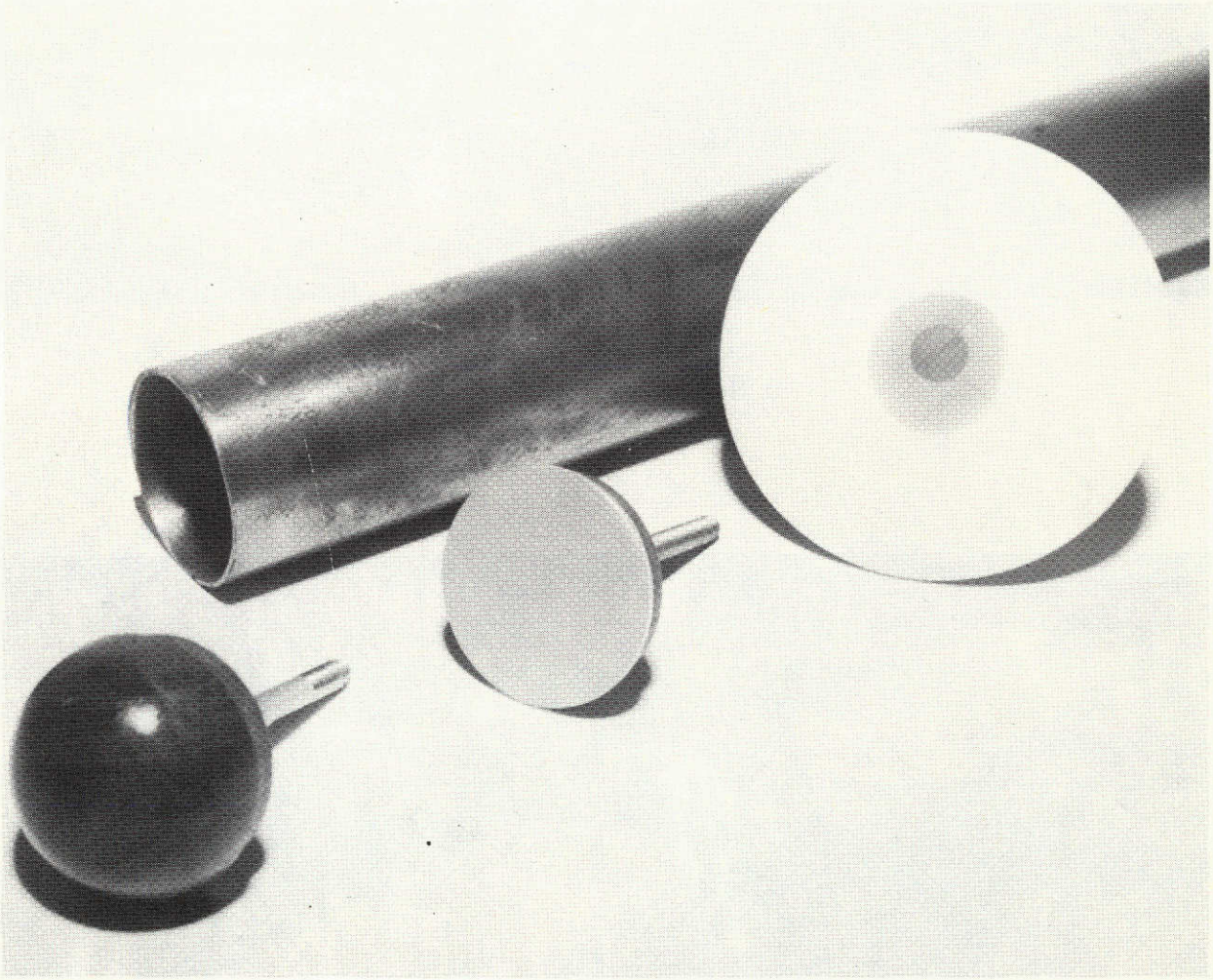

L-70-2679.1

Figure 1.- Photograph of cylindrical blade tip and blade-tip shapes tested.

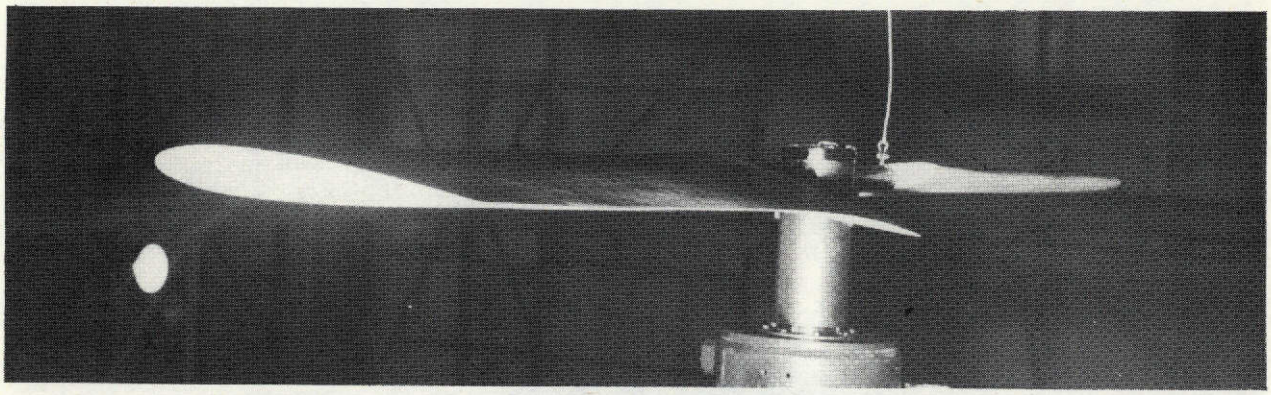

L-70-2685

(a) Helically twisted blade.

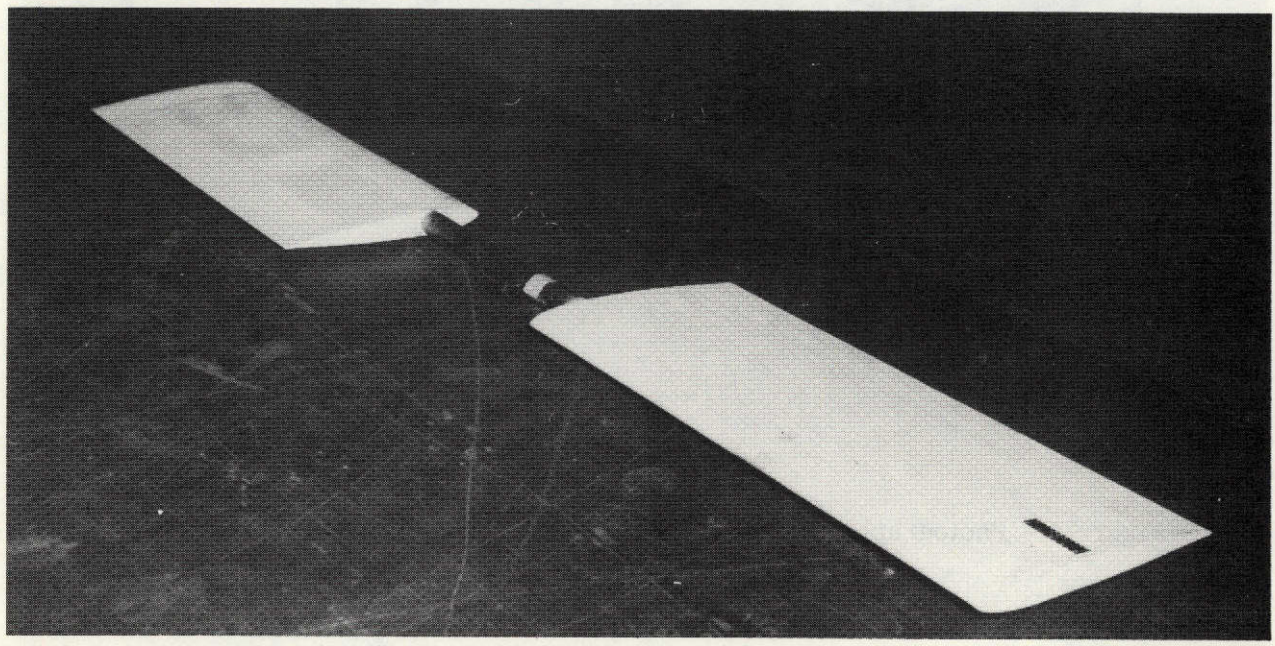

L-70-2682

(b) Untwisted blade.

Figure 2.- Rotor with airfoil blades with and without twist.

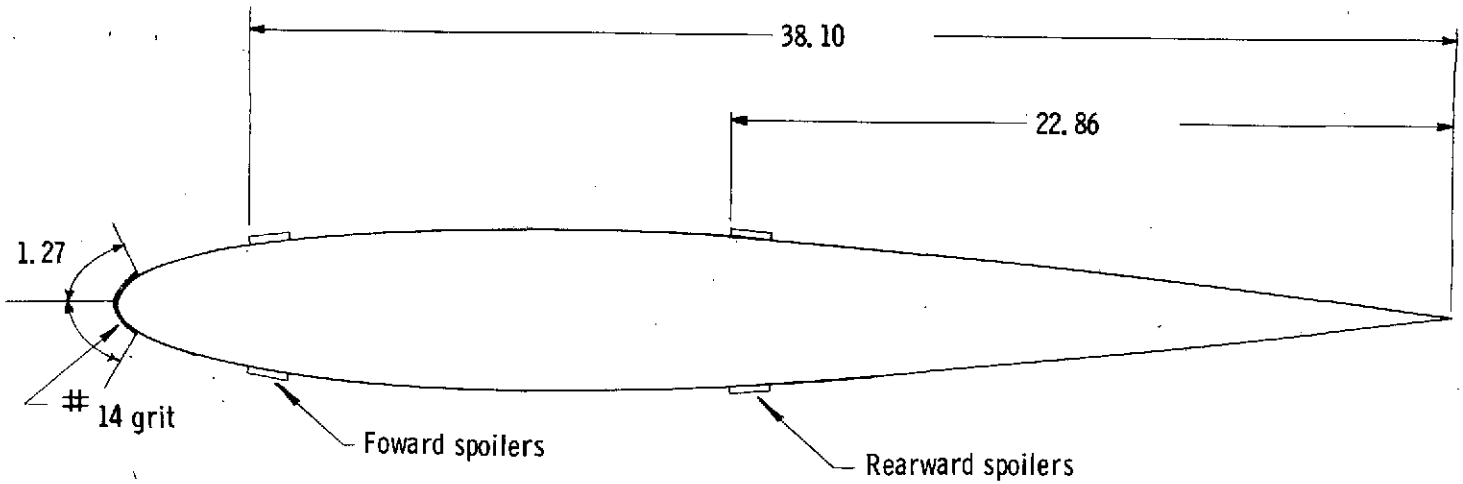

(a) Airfoil blade with grit and spoilers. Configuration 14.

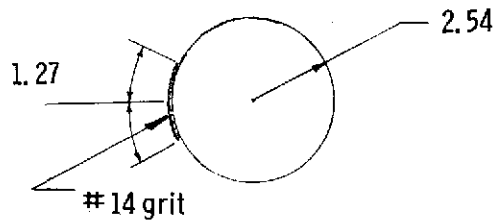

(b) Circular blade section with No. 14 grit. Configuration 03.

Figure 3.- Blade cross sections indicating the location of the grit and the spoilers. All dimensions are in centimeters.

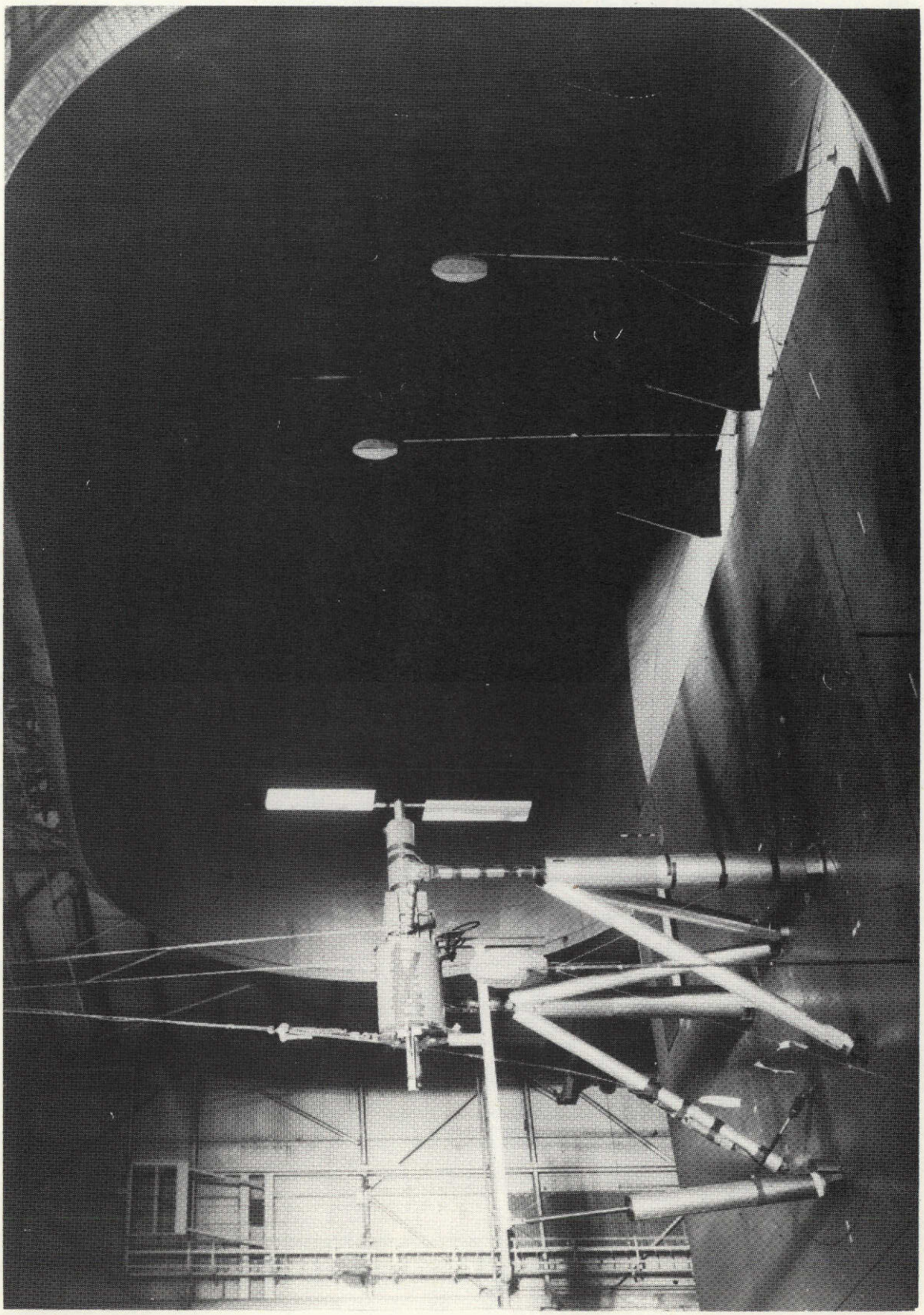

L-71-632

Figure 4.- Test setup in Langley full-scale tunnel.

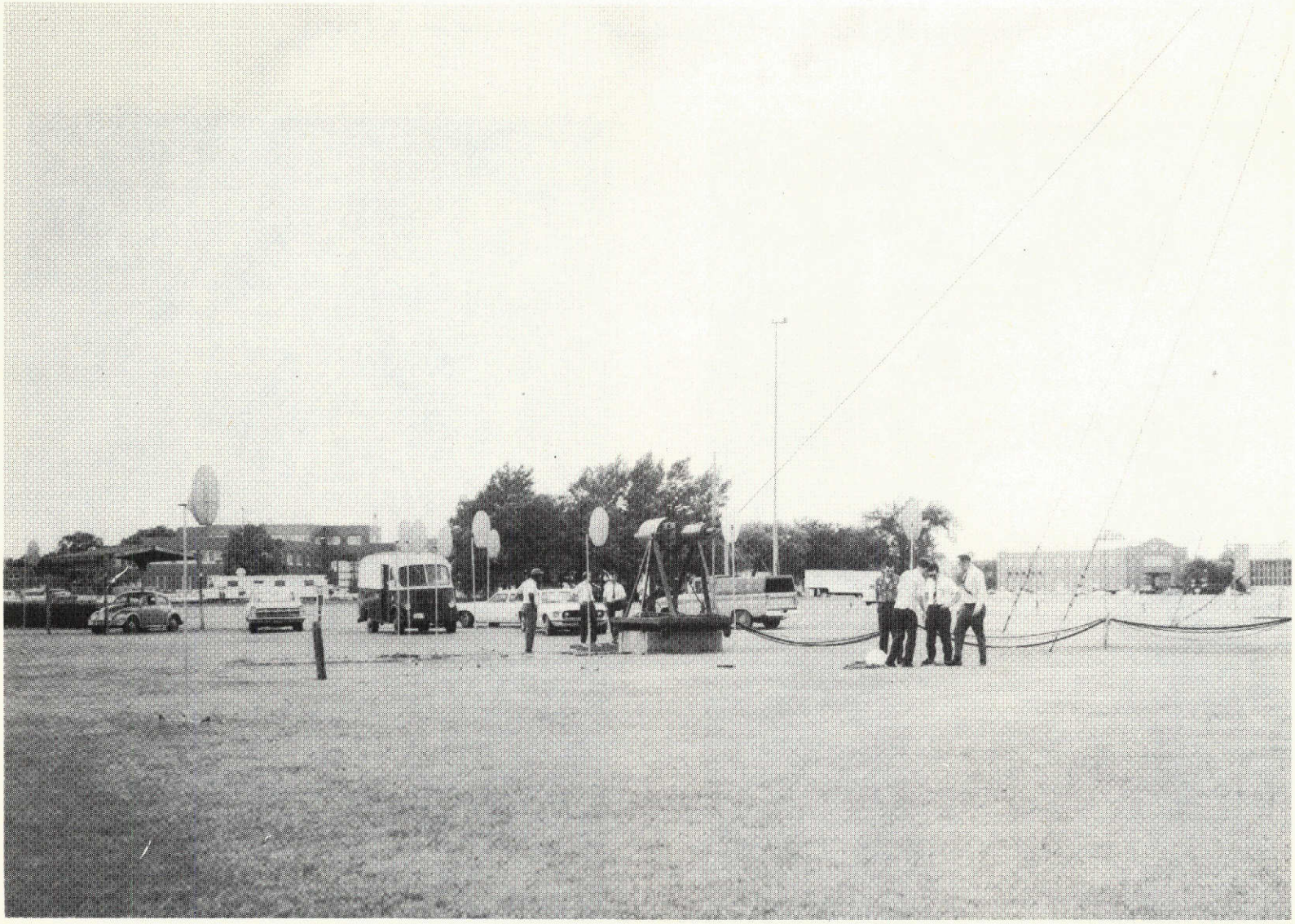

L-71-633

Figure 5.- Test setup for free field.

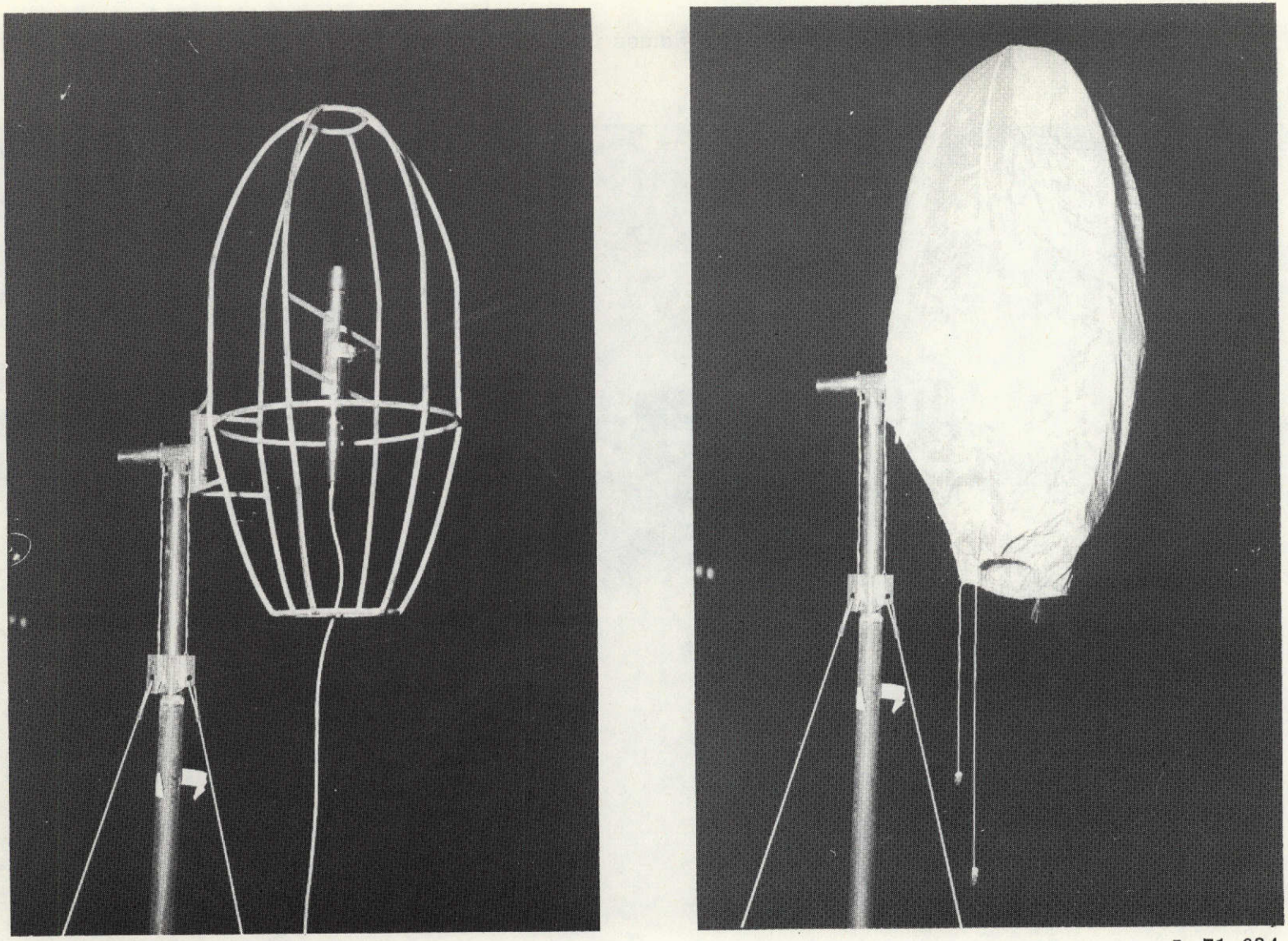

L-71-634

Figure 6.- Microphone, microphone support, and wind screen.

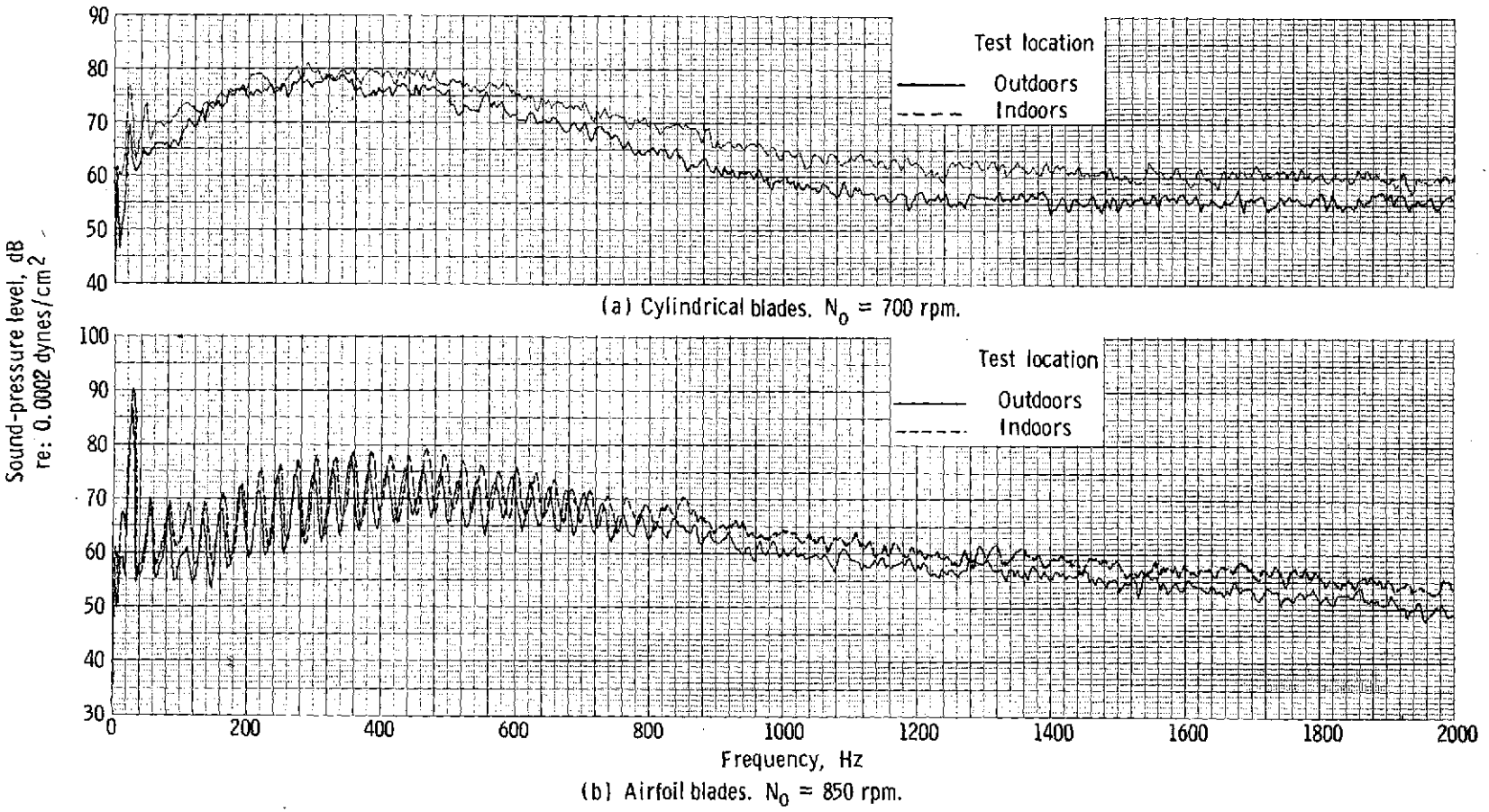

Figure 7.- Effect of wind-tunnel reverberation. Microphone located at 2-diameter distance along rotational axis.

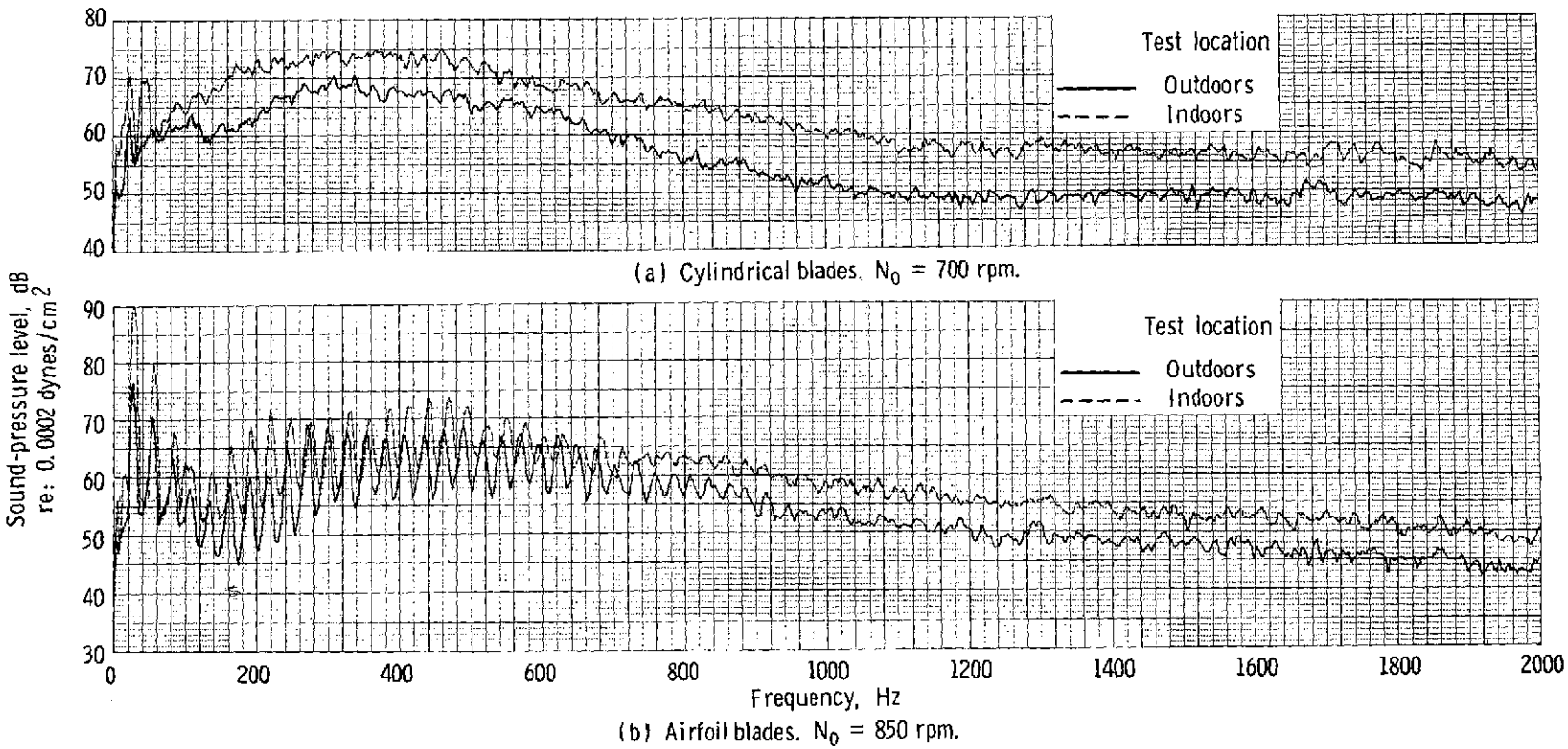

Figure 8.- Effect of wind-tunnel reverberation. Microphone located at 5.5-diameter distance along rotational axis.

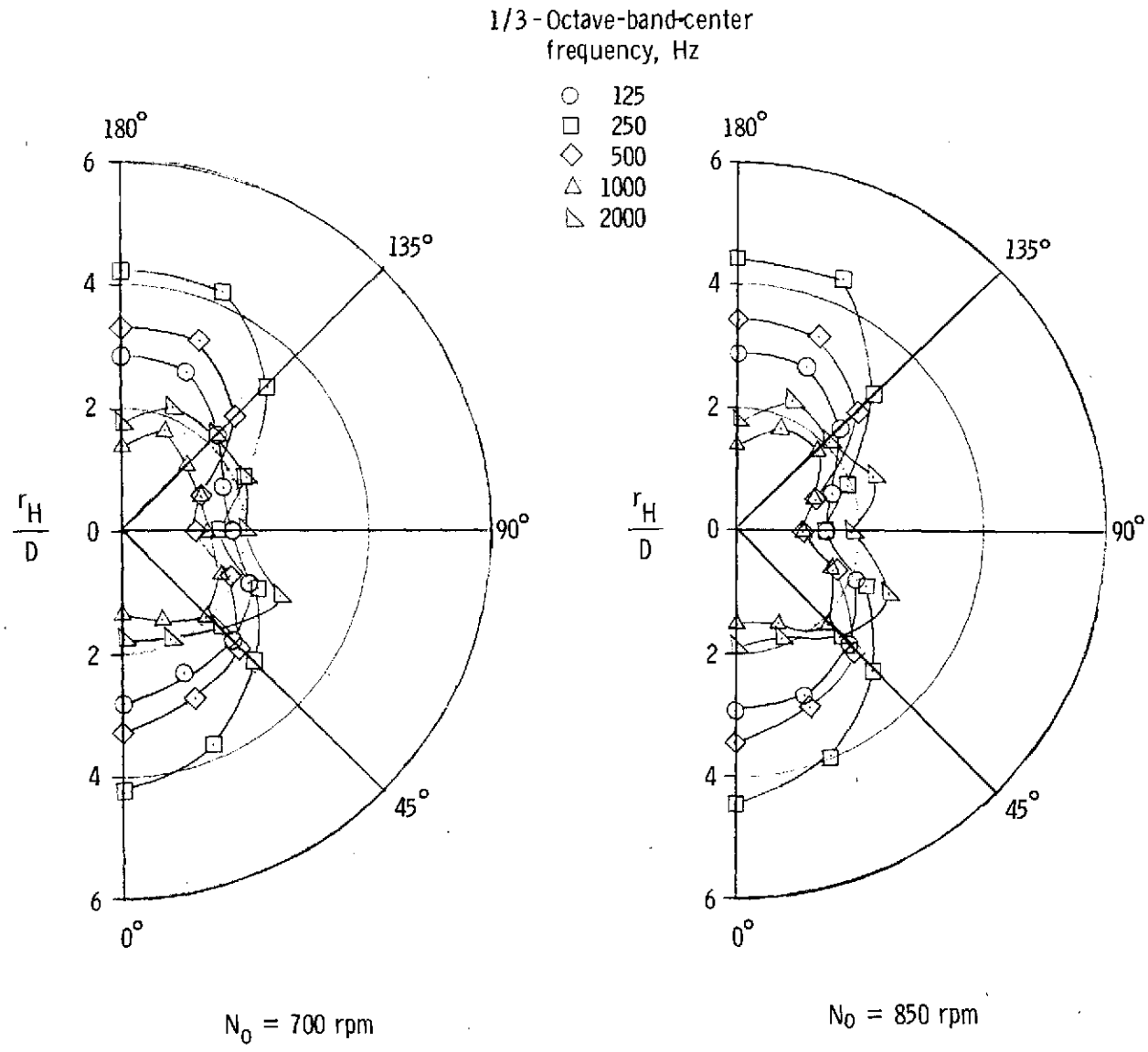

Figure 9.- Hall radius for rotor with cylindrical blades.

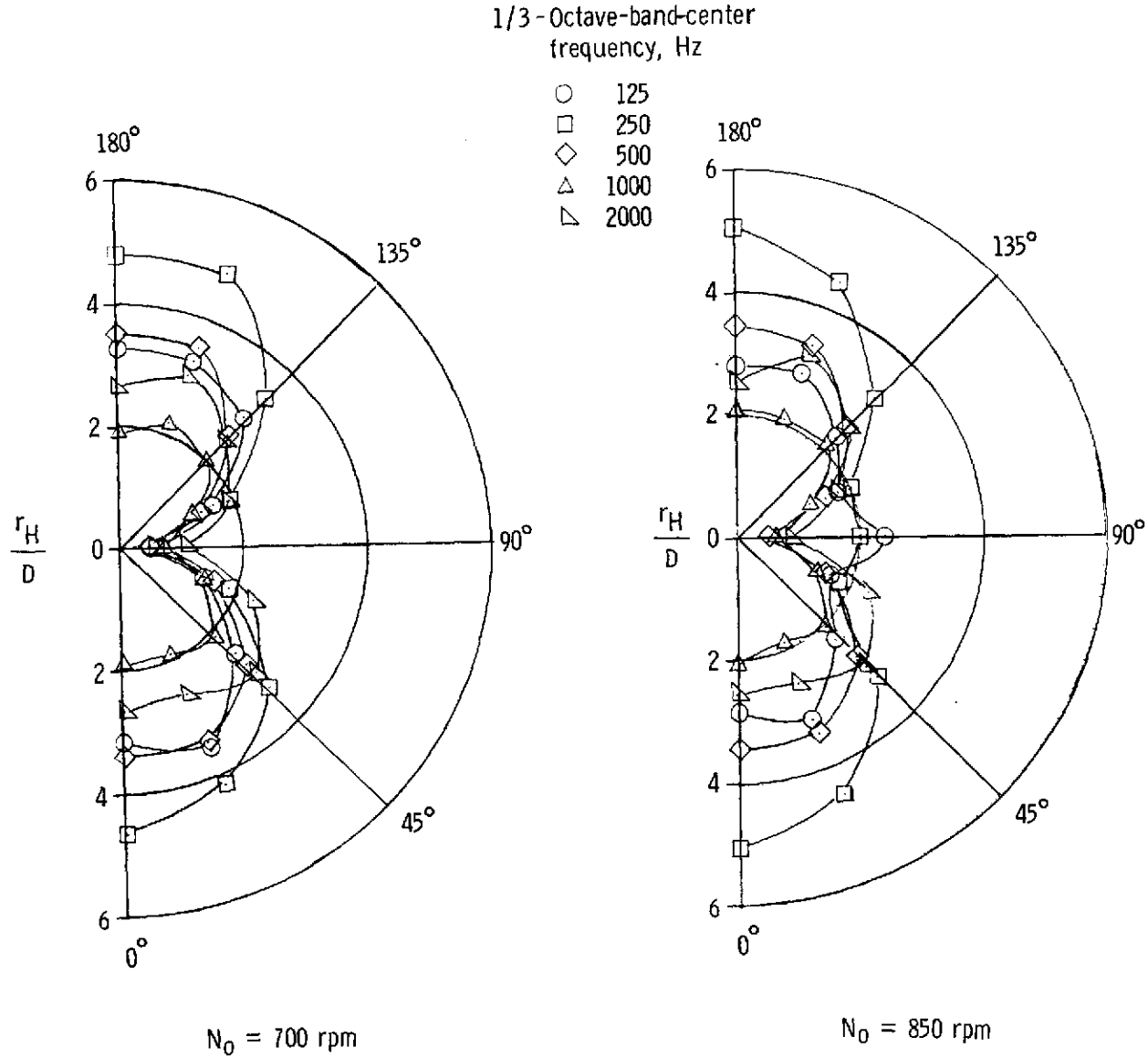

Figure 10.- Hall radius for rotor with airfoil blades.

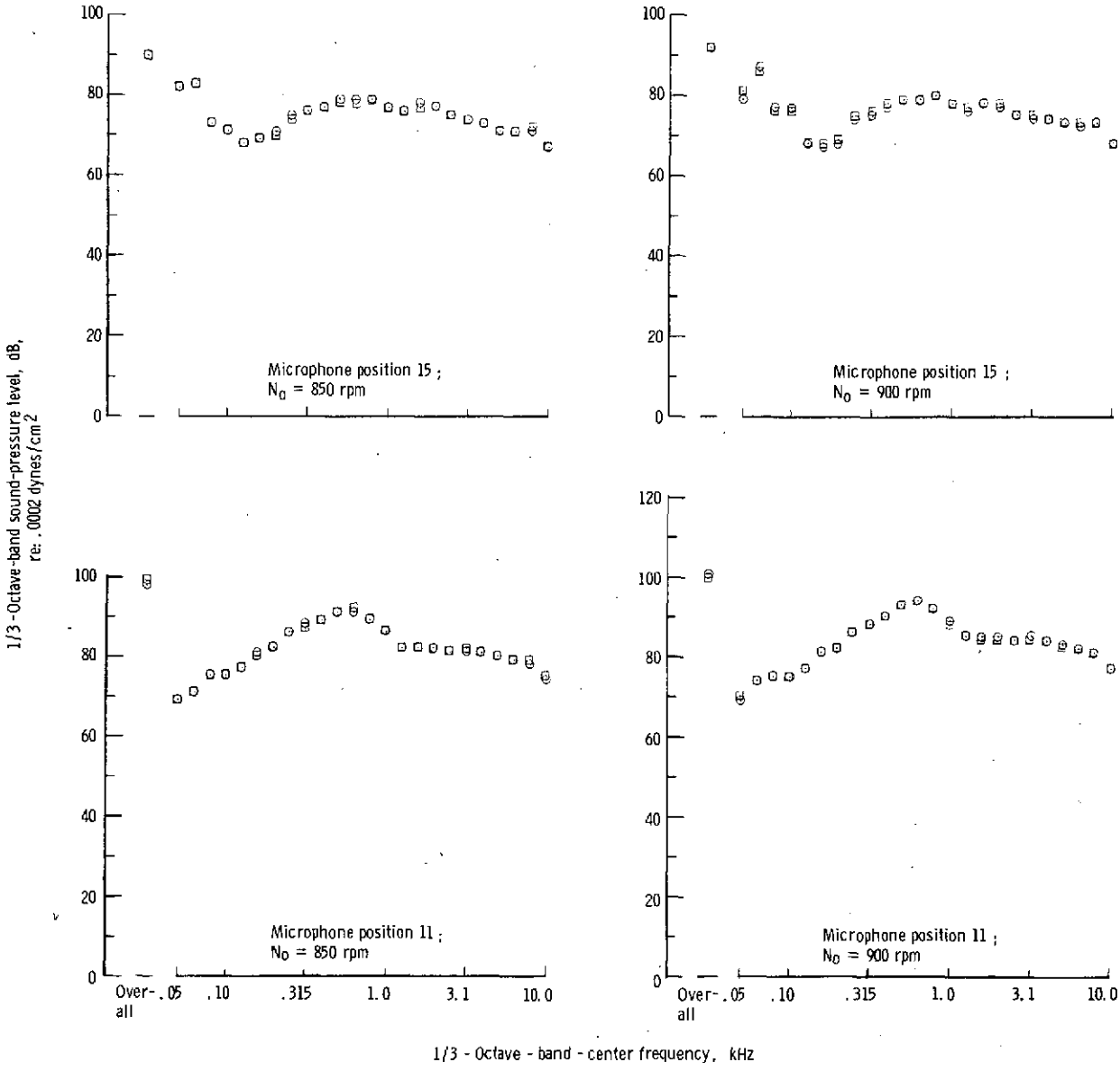

Figure 11.- Data repeatability.

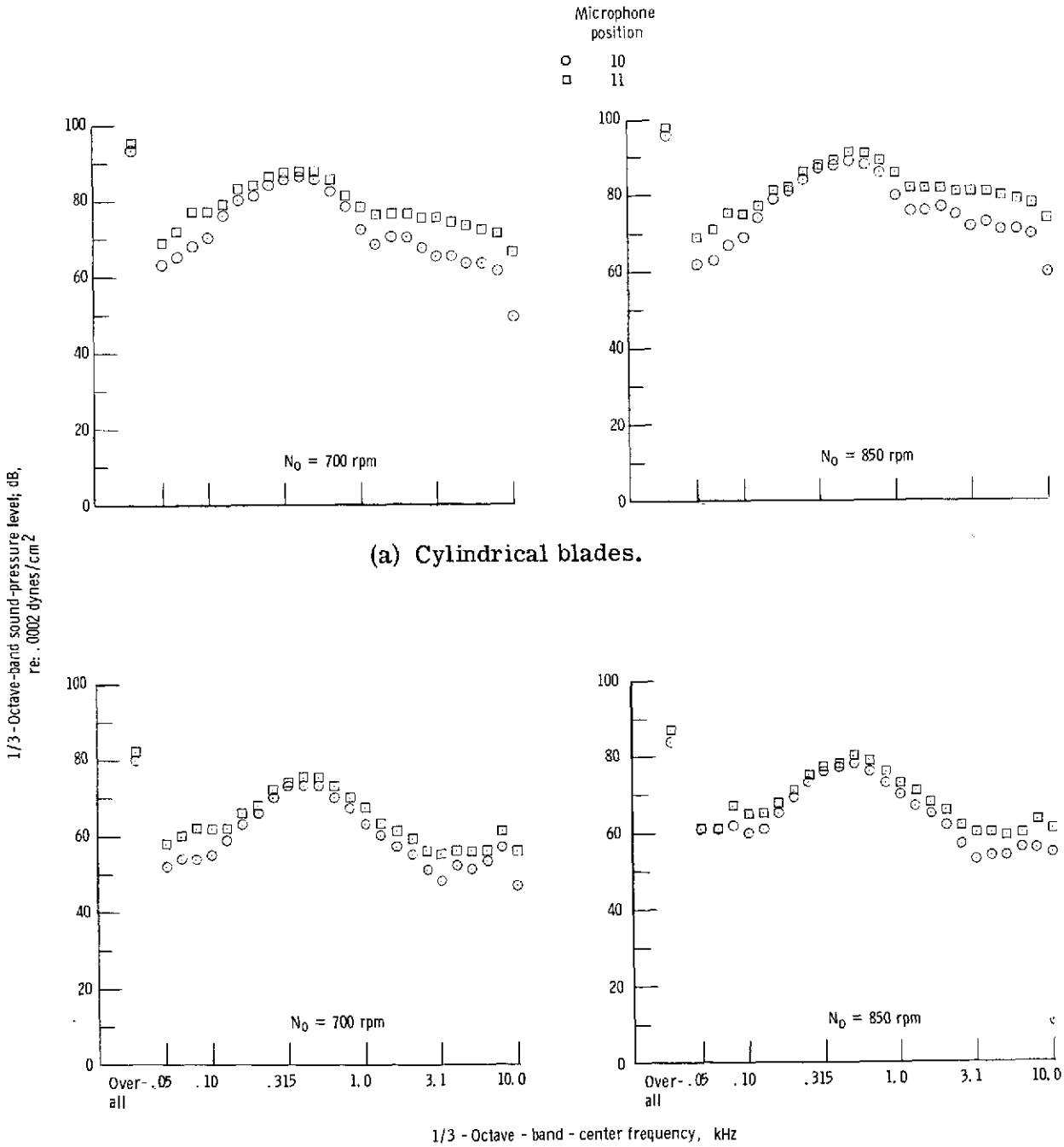

(a) Cylindrical blades.

(b) Airfoil blades.

Figure 12.- Evaluation of ground reflectivity in outdoor tests.

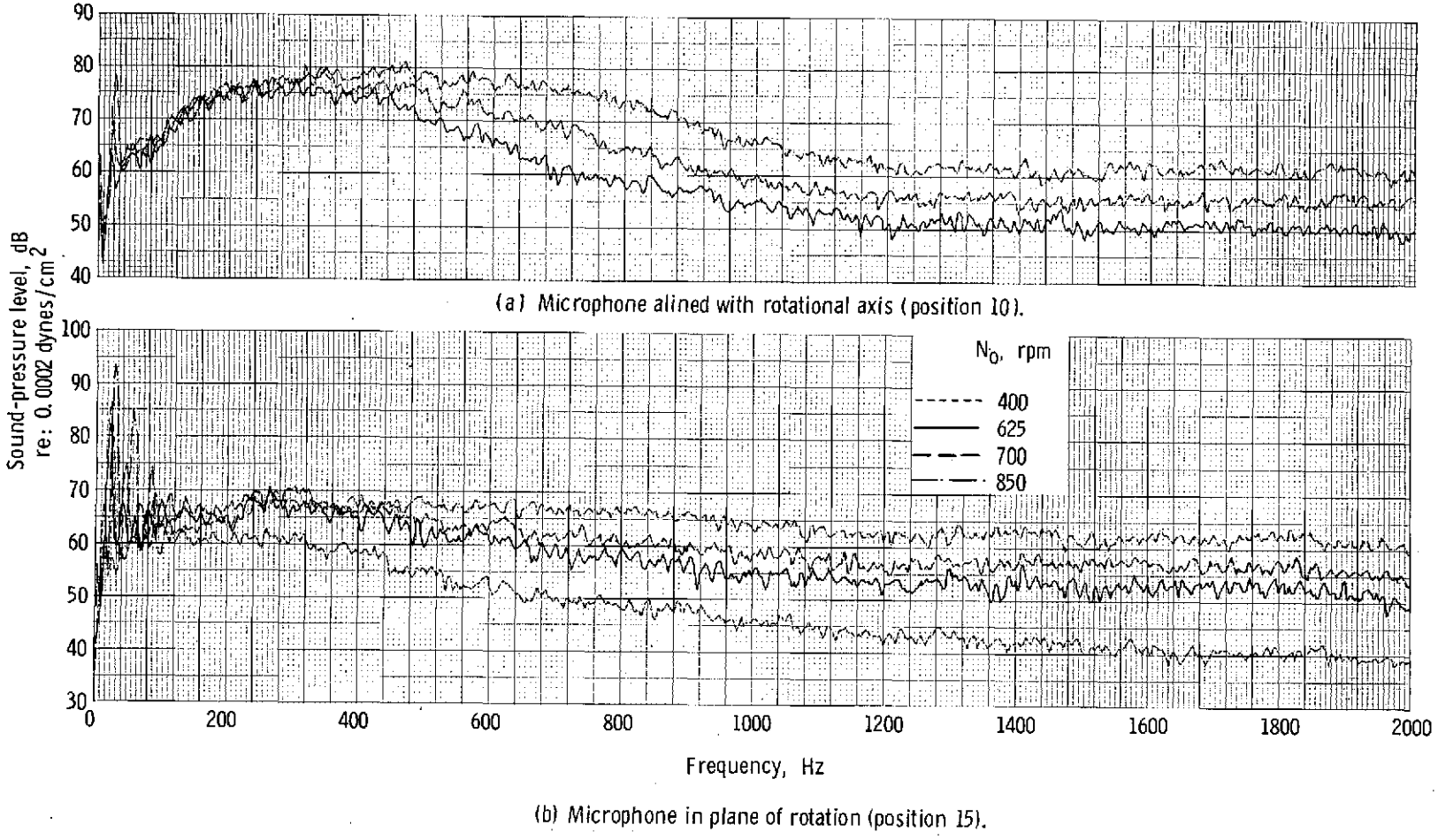

(a) Microphone alined with rotational axis (position 10).

(b) Microphone in plane of rotation (position 15).

Figure 13.- Amplitude-frequency spectra for rotor with cylindrical blades. V = 0.

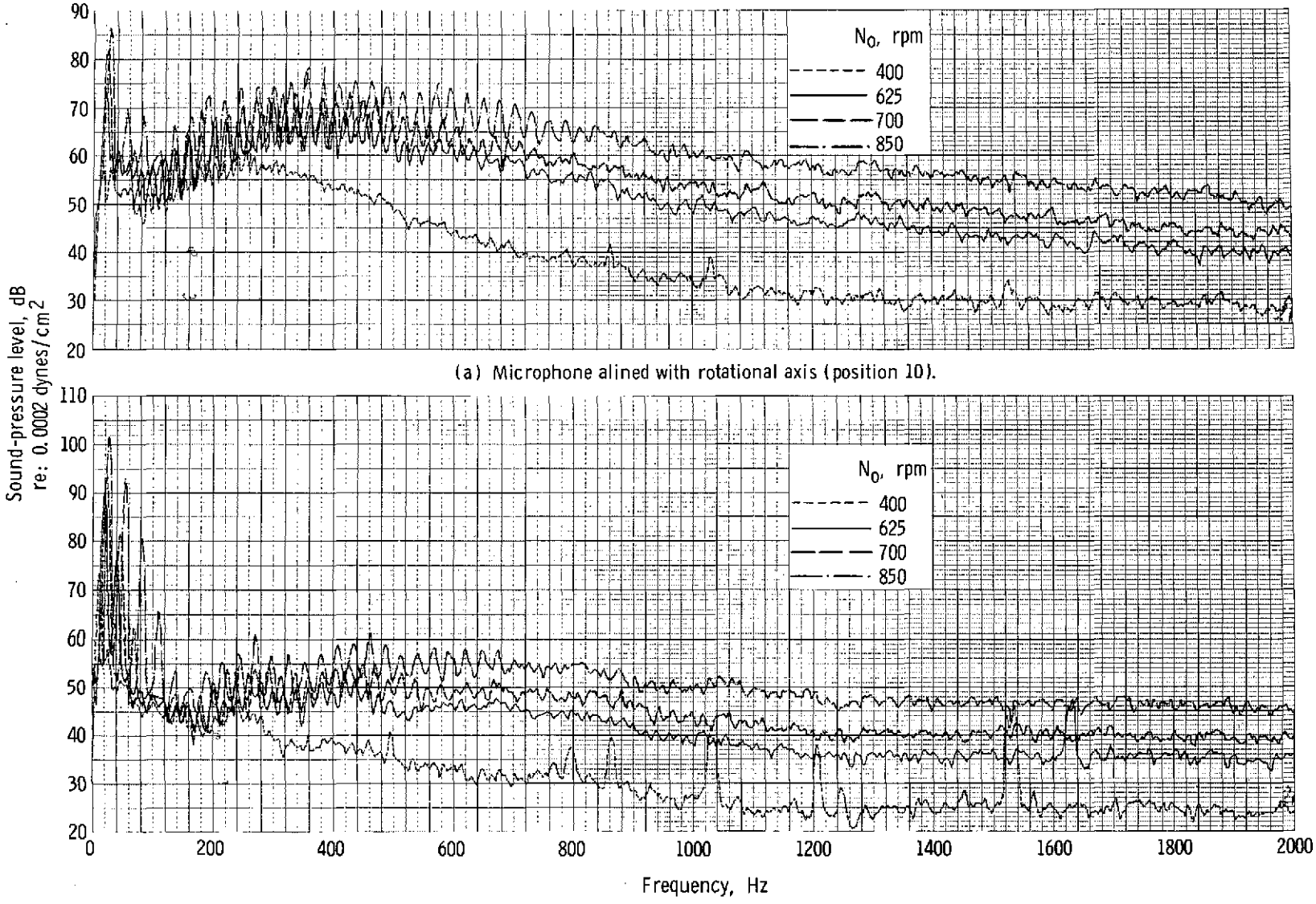

(a) Microphone alined with rotational axis (position 10).

(b) Microphone in plane of rotation (position 15).

Figure 14.- Amplitude-frequency spectra for rotor with airfoil blades. V = 0.

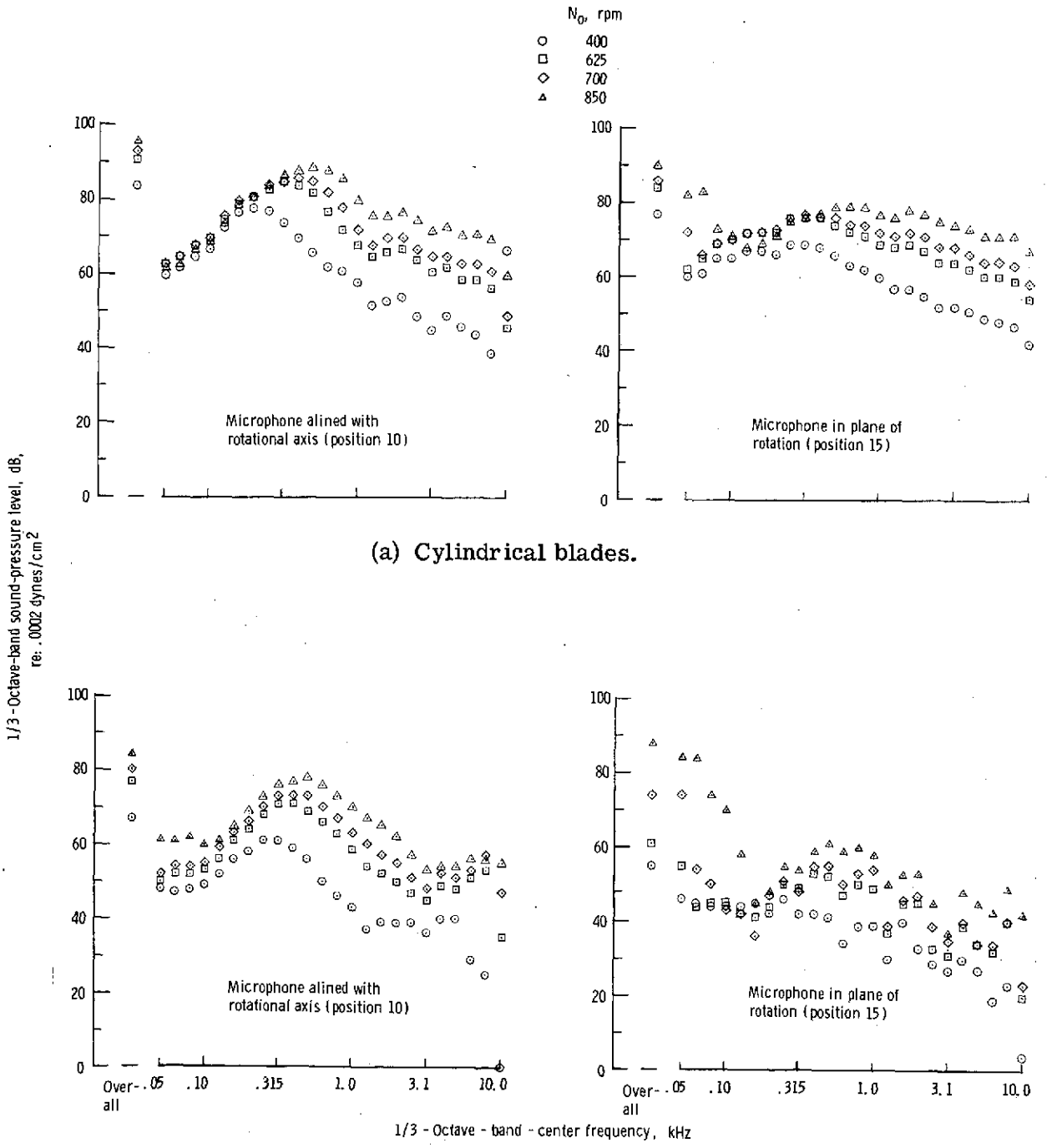

(a) Cylindrical blades.

(b) Airfoil blades.

Figure 15.- Comparison of amplitude-frequency spectra along rotor axis and in plane of rotation. V = 0.

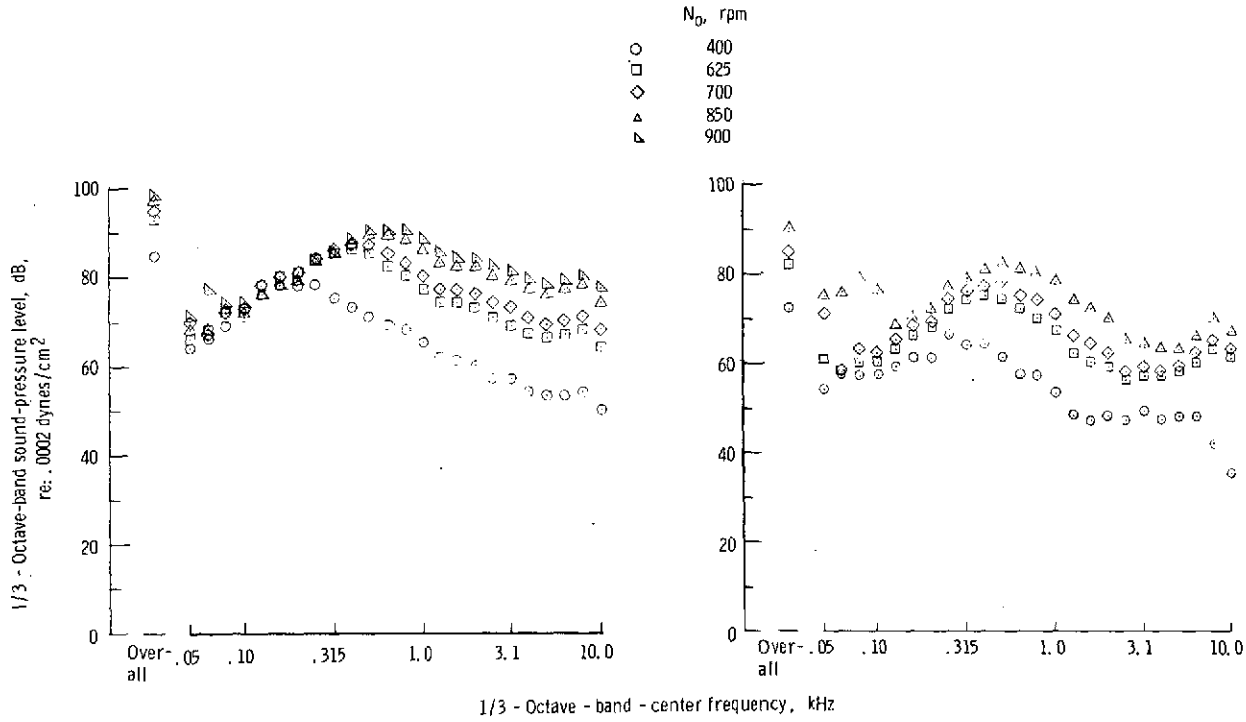

(a) Cylindrical blades. (b) Airfoil blades.

Figure 16.- Amplitude-frequency spectra measured at 45° to rotational axis (microphone position 1). V = 0.

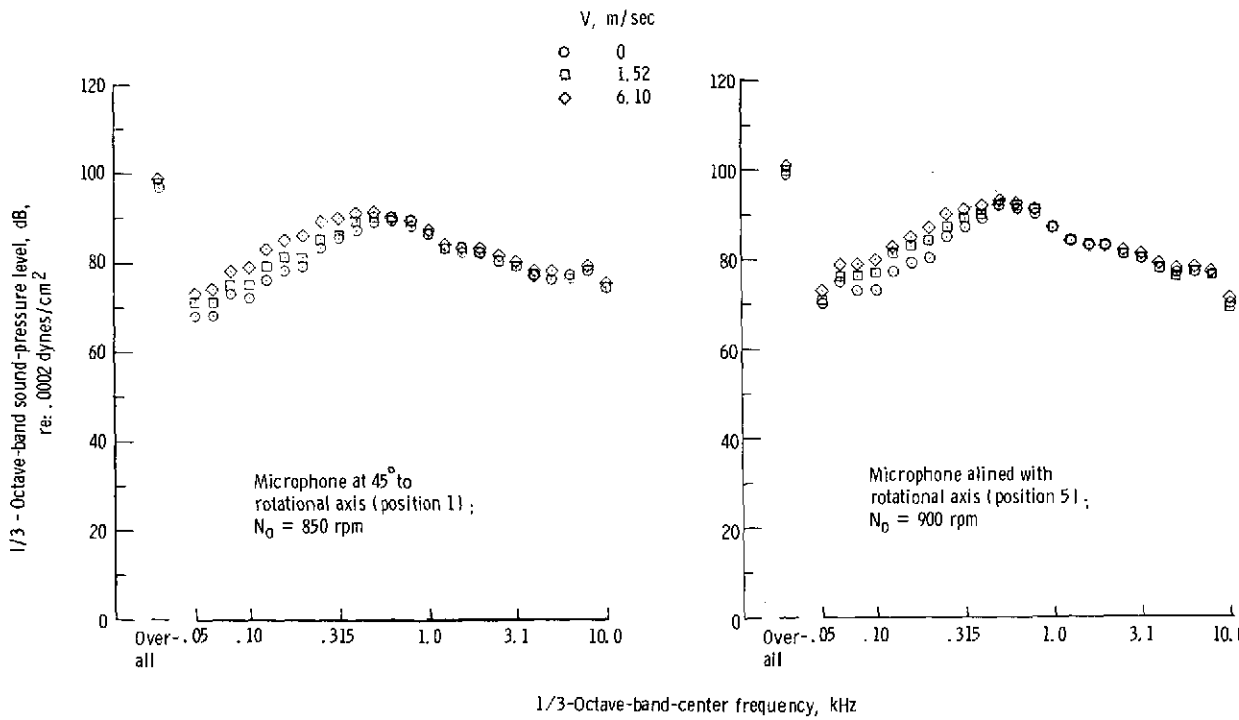

Figure 17.- Wind-tunnel forward-speed effects for rotor with cylindrical blades.

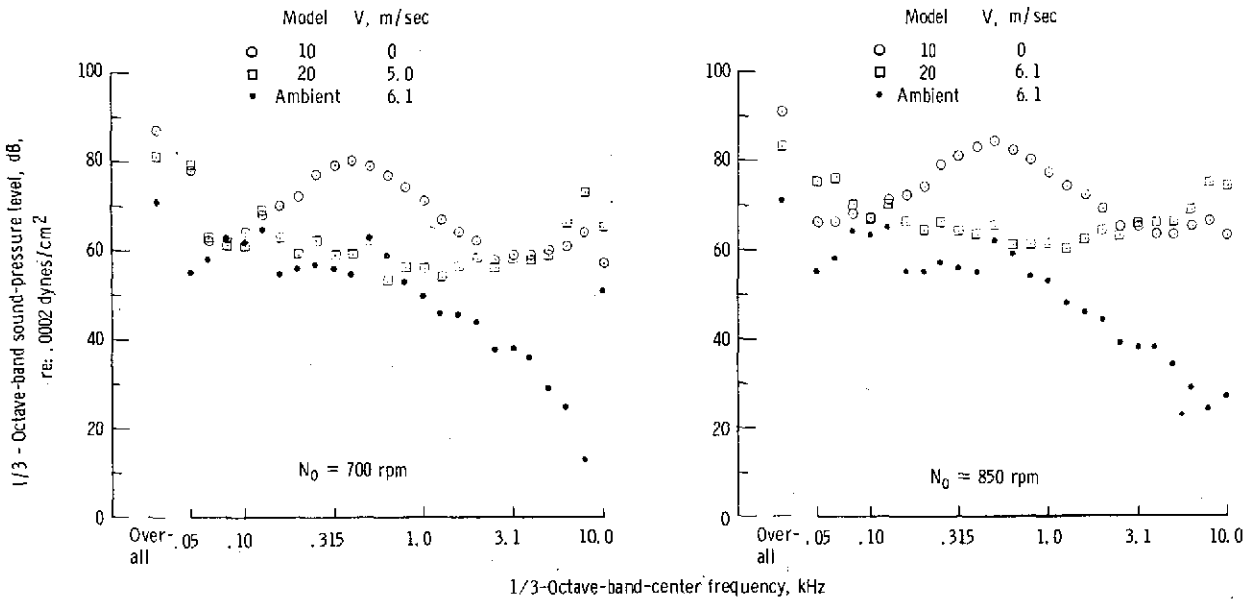

(a) Microphone alined with rotational axis (position 5).

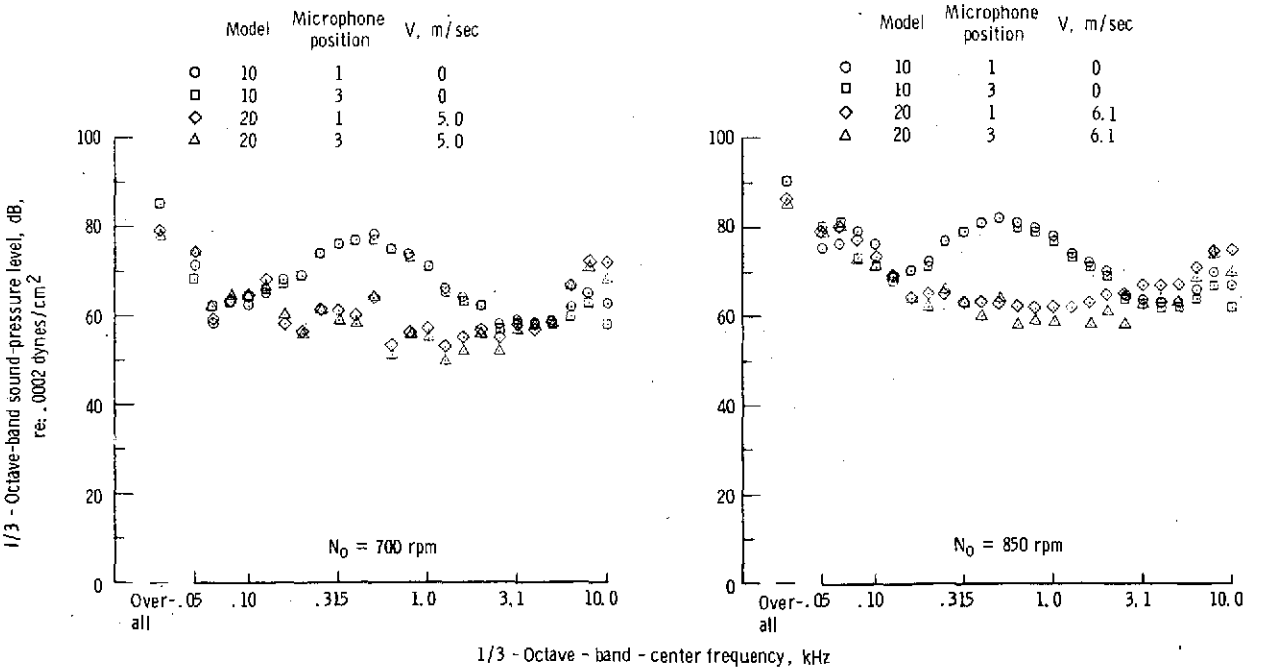

(b) Microphone at 45° to rotational axis.

Figure 18.- Wind-tunnel forward-speed effects for rotor with airfoil blades.

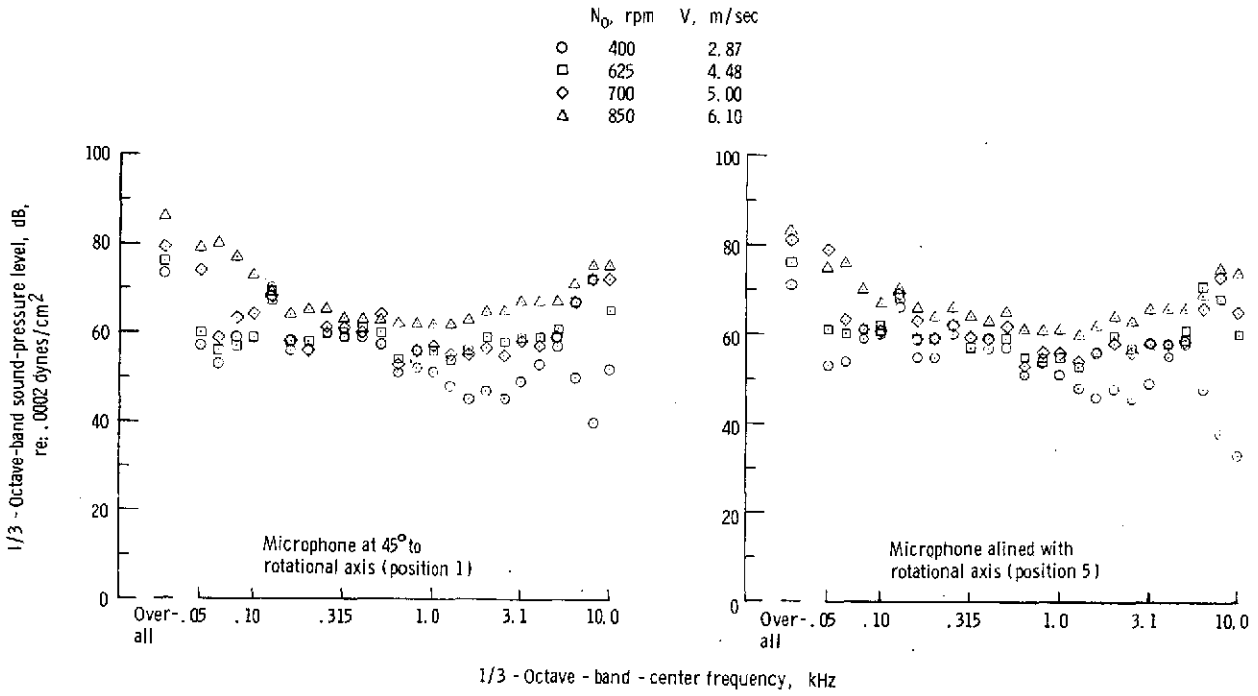

Figure 19.- Wind-tunnel forward-speed effects for rotor with airfoil blades.

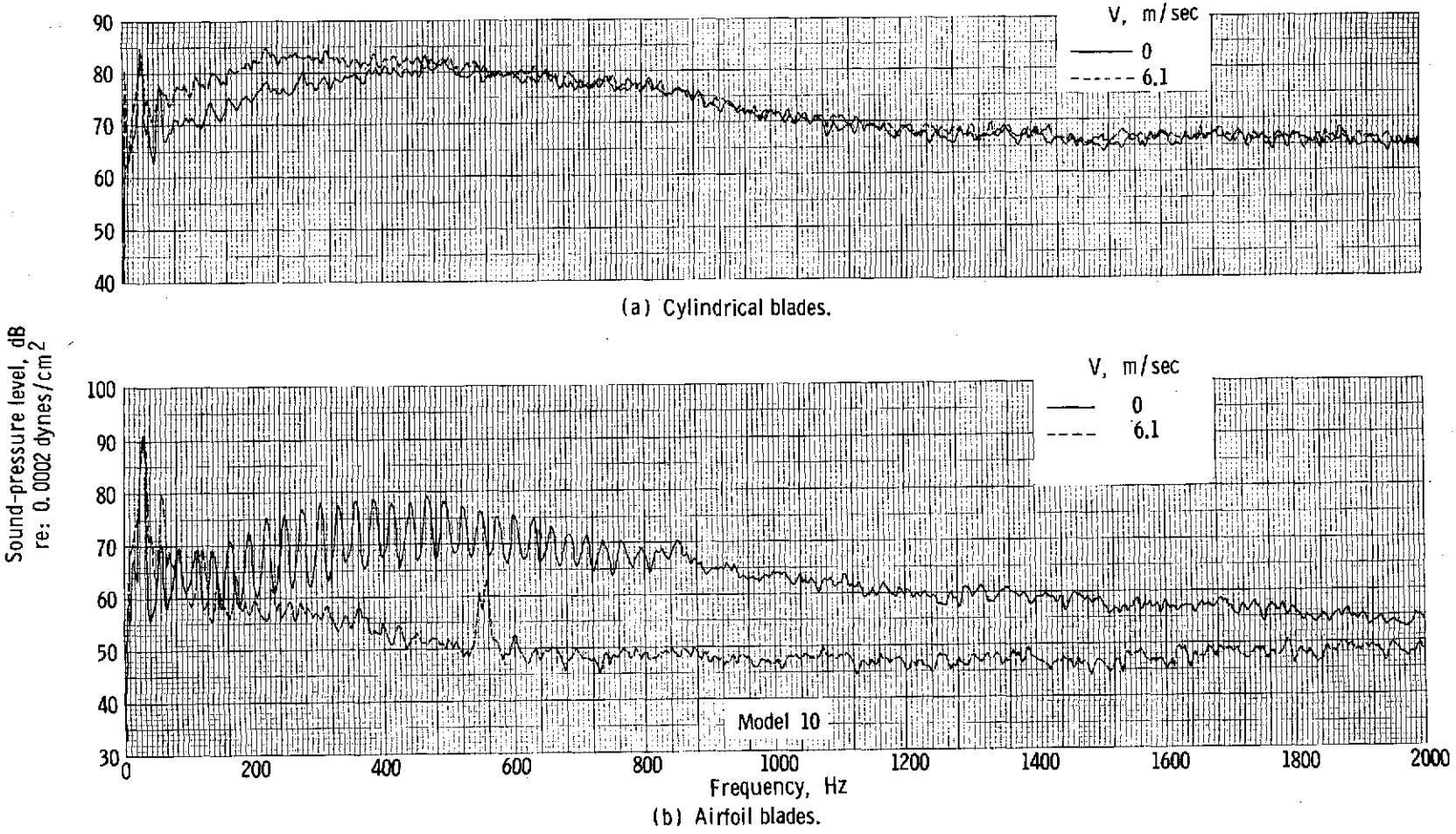

Figure 20.- Effect of forward speed for two different blade sections. Microphone alined with rotational axis (position 5). N_0 = 850 rpm.

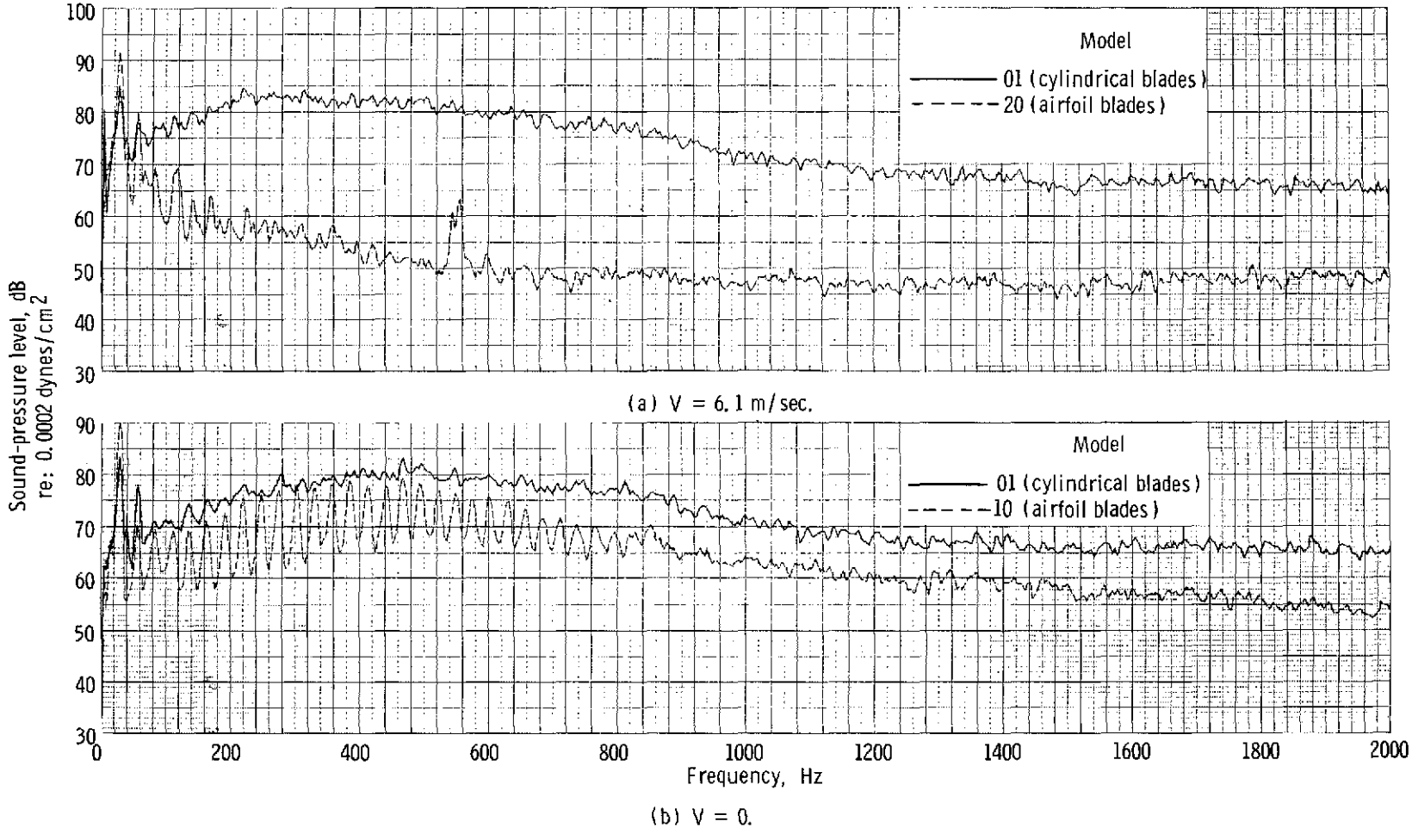

Figure 21.- Effect of blade section, with and without forward speed.
Microphone position 5; N_0 = 850 rpm.

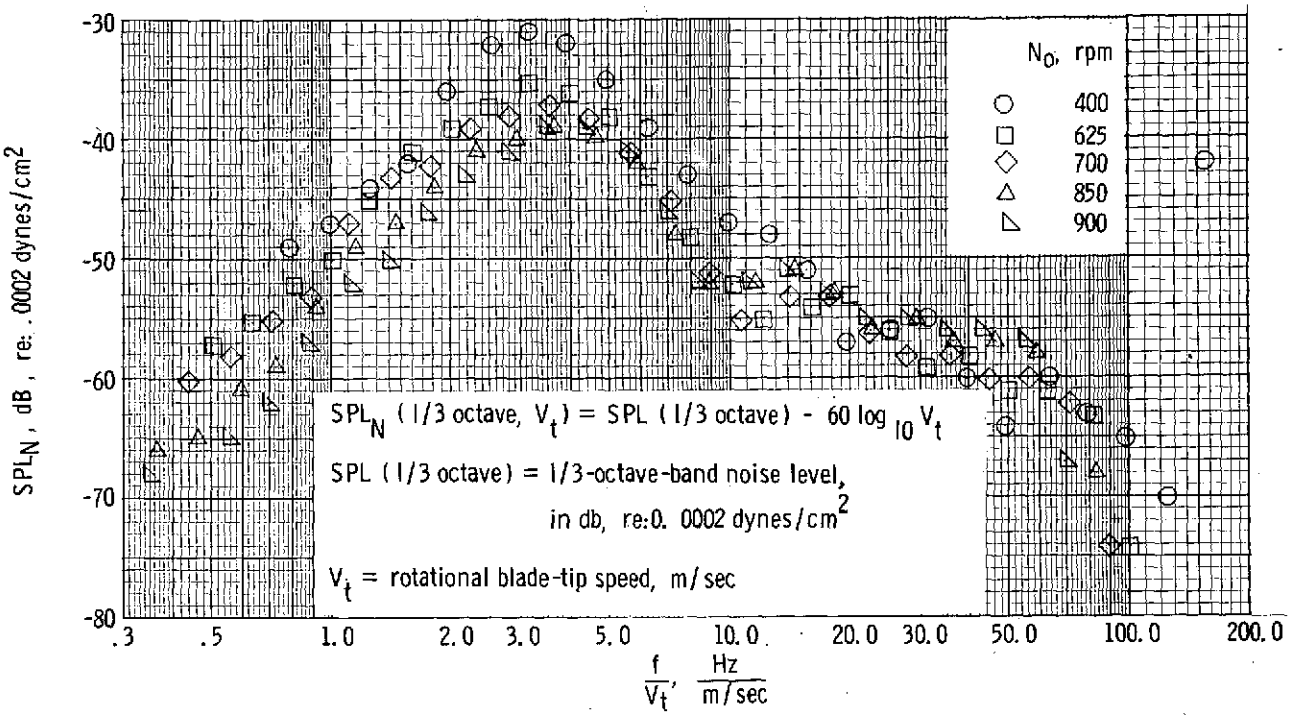

(a) Microphone alined with rotational axis (position 10).

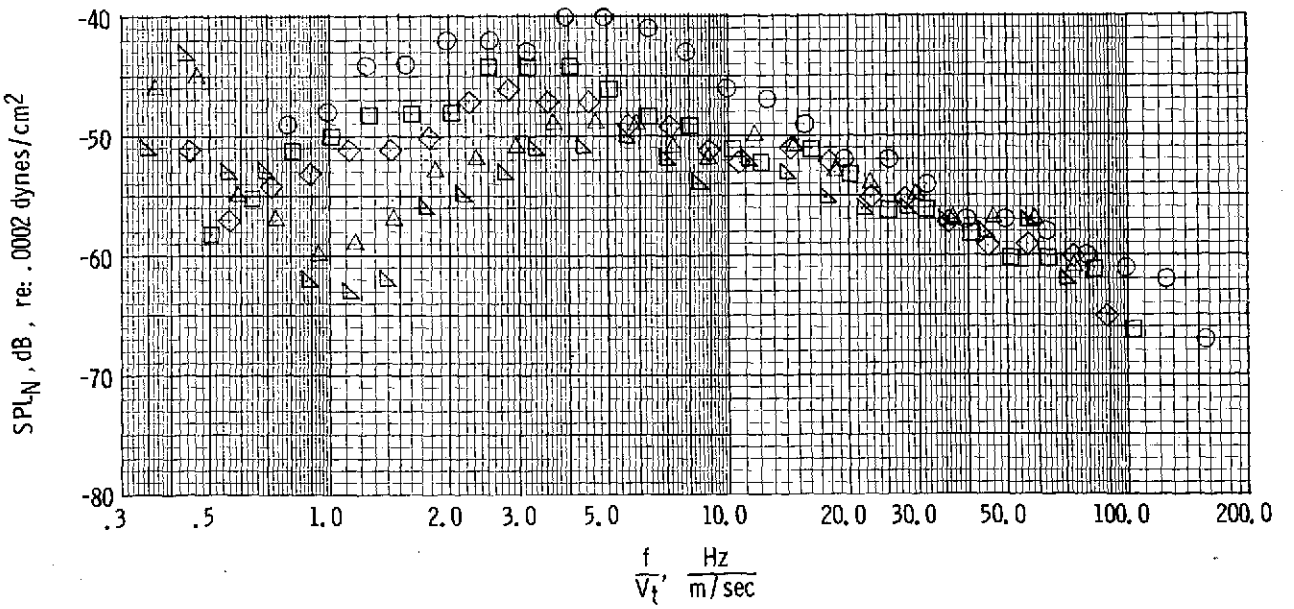

(b) Microphone in plane of rotation (position 15).

Figure 22.- Scaling of noise spectra for rotor with cylindrical blades at $V = 0$.

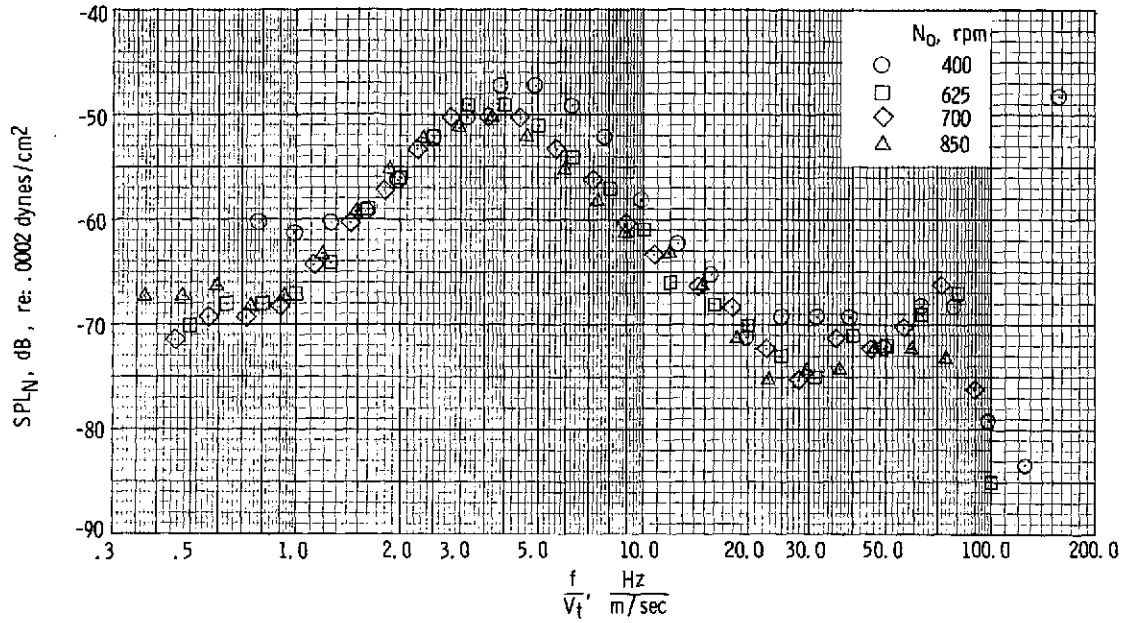

(a) Microphone alined with rotational axis (position 10).

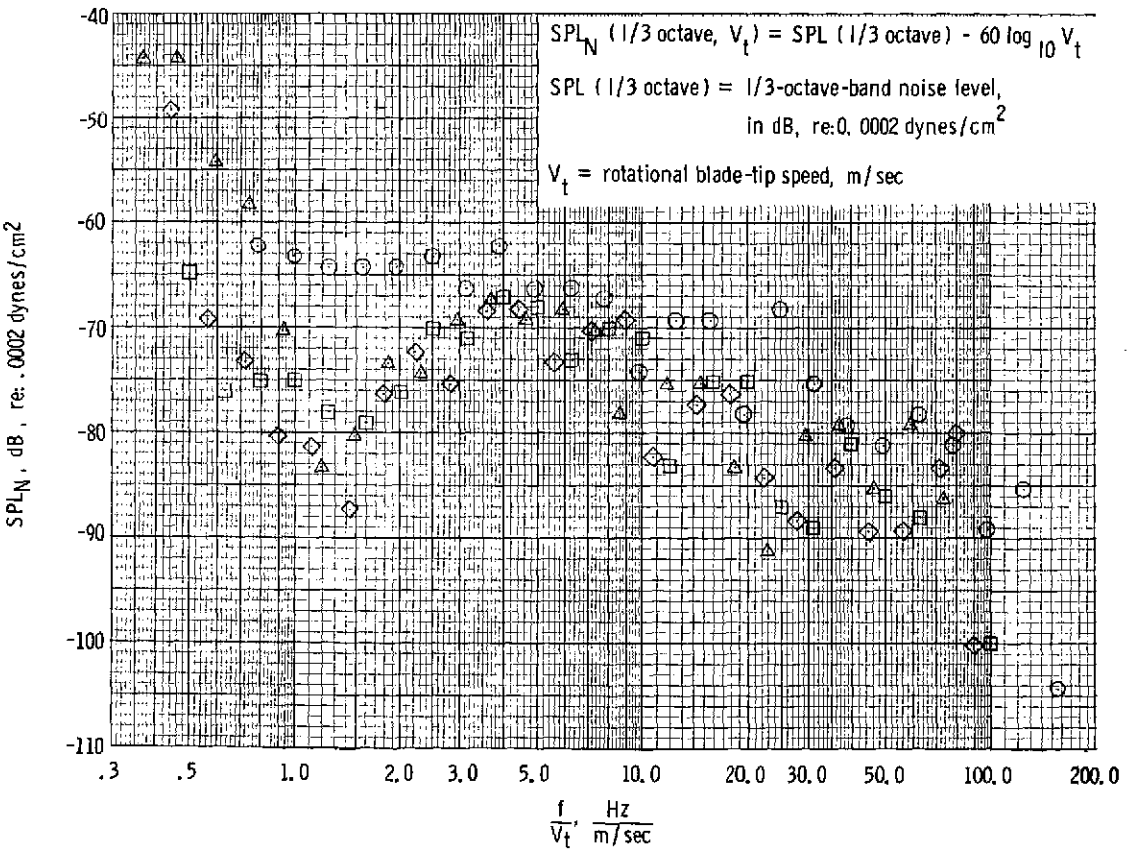

(b) Microphone in plane of rotation (position 15).

Figure 23.- Scaling of noise spectra for rotor with airfoil blades at $V = 0$.

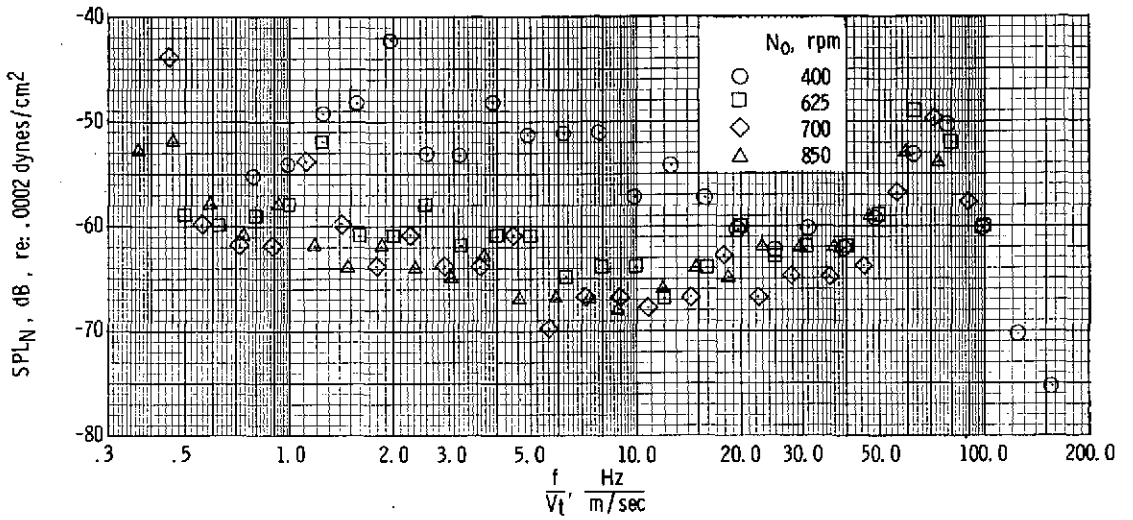

(a) Microphone alined with rotational axis (position 5).

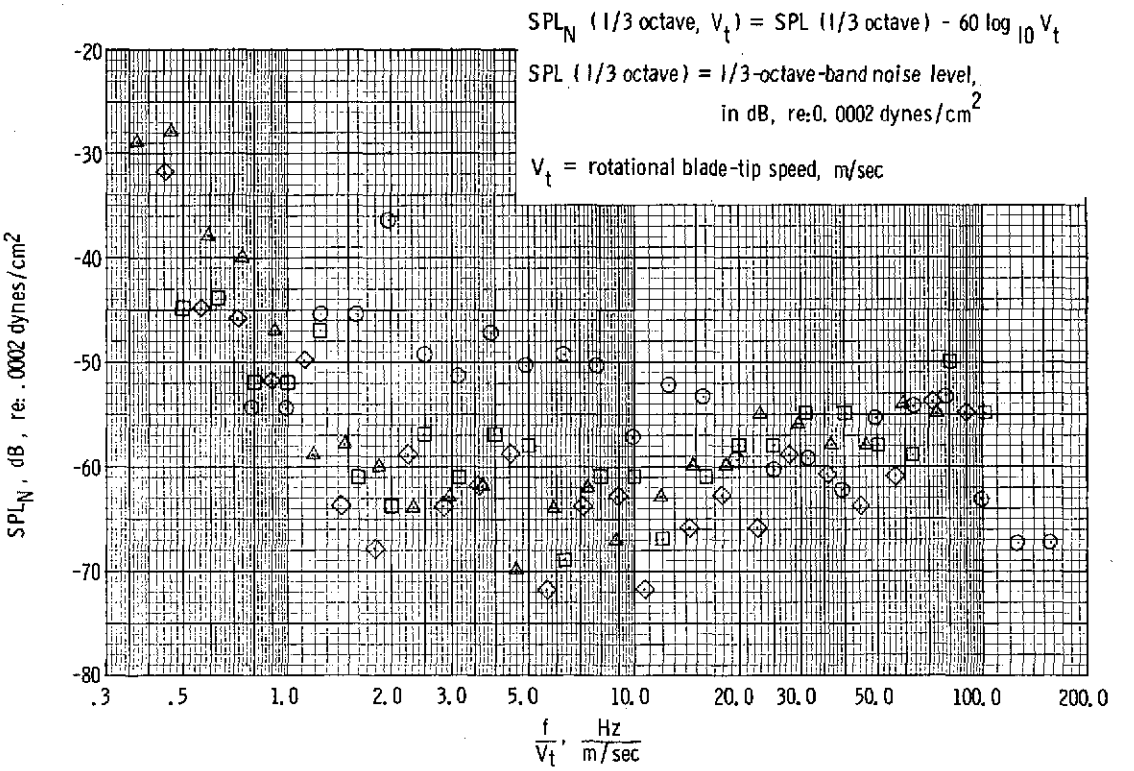

(b) Microphone in plane of rotation (position 2).

Figure 24.- Scaling of noise spectra for rotor with airfoil blades with wind on. V = Variable.

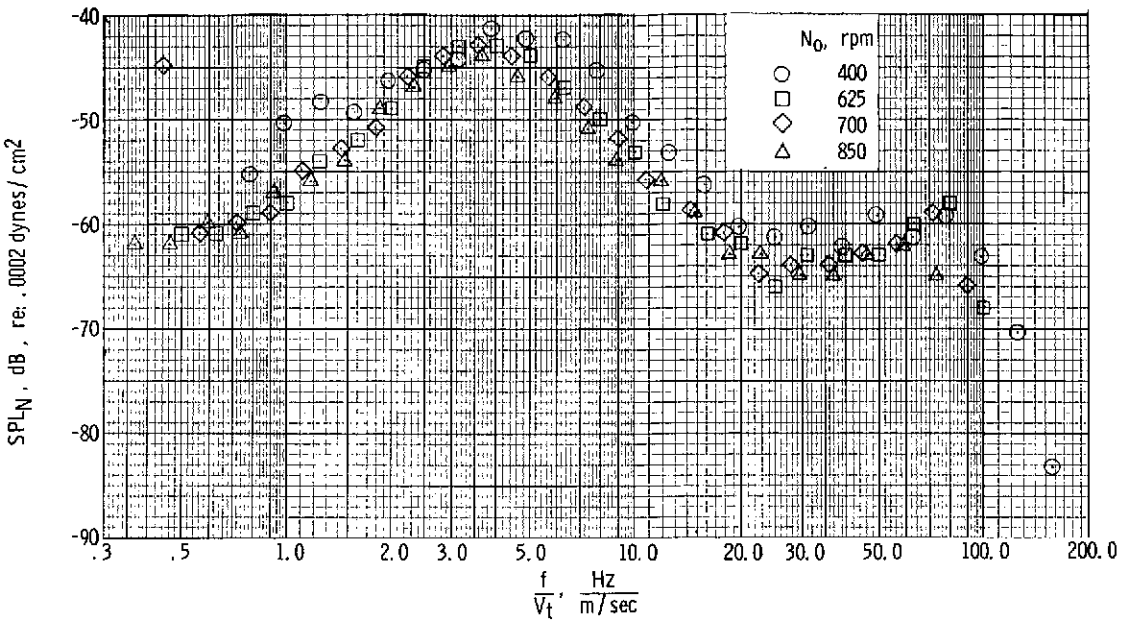

(a) Microphone alined with rotational axis (position 5).

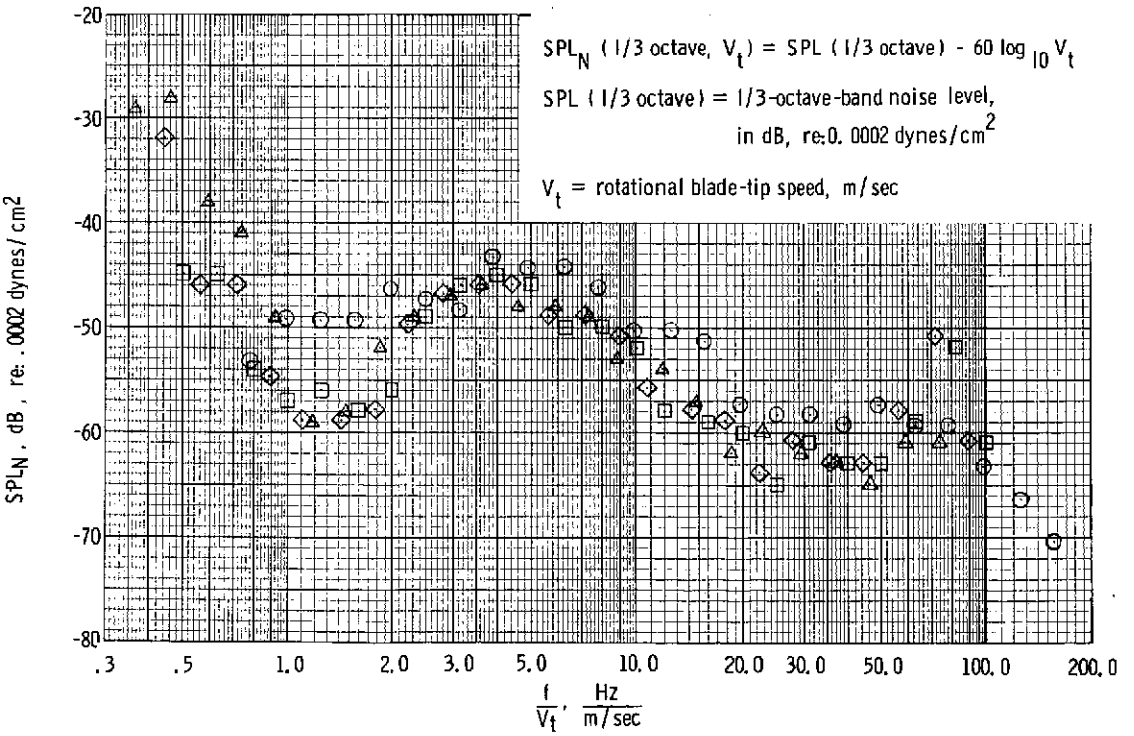

(b) Microphone in plane of rotation (position 2).

Figure 25.- Scaling of noise spectra for rotor with airfoil blades at $V = 0$.

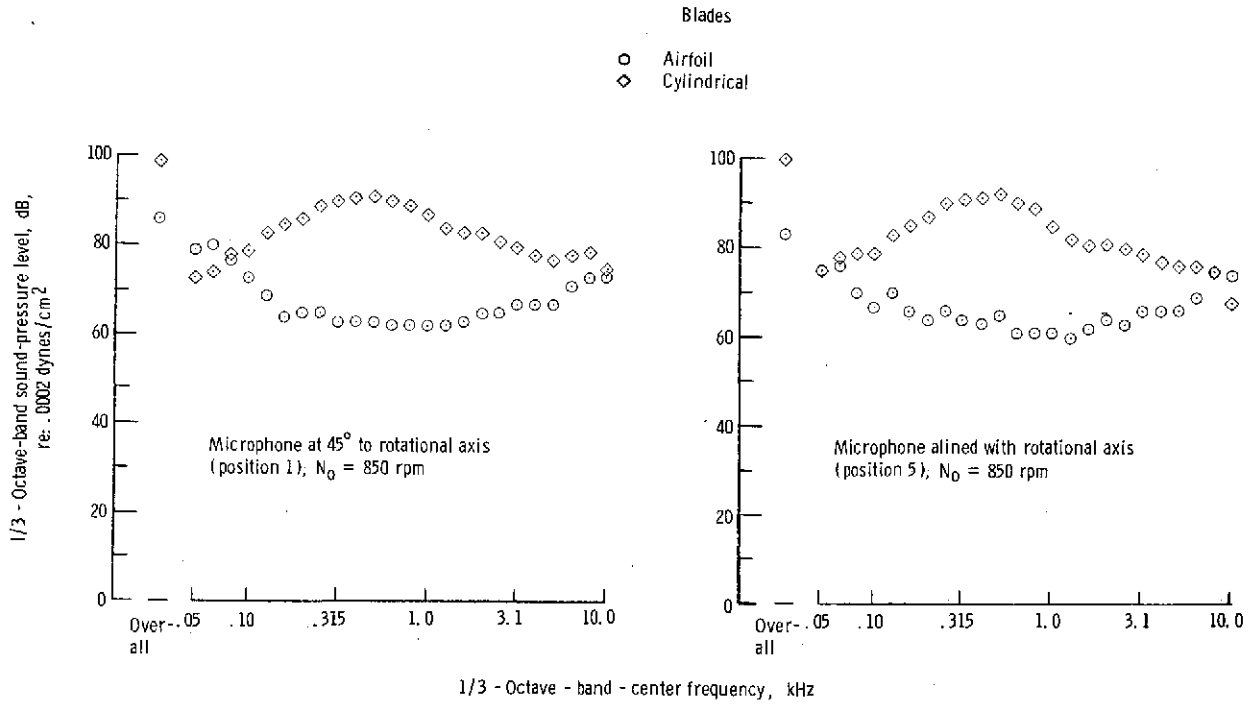

Figure 26.- Effect of blade section with wind on. V = 6.1 m/sec.

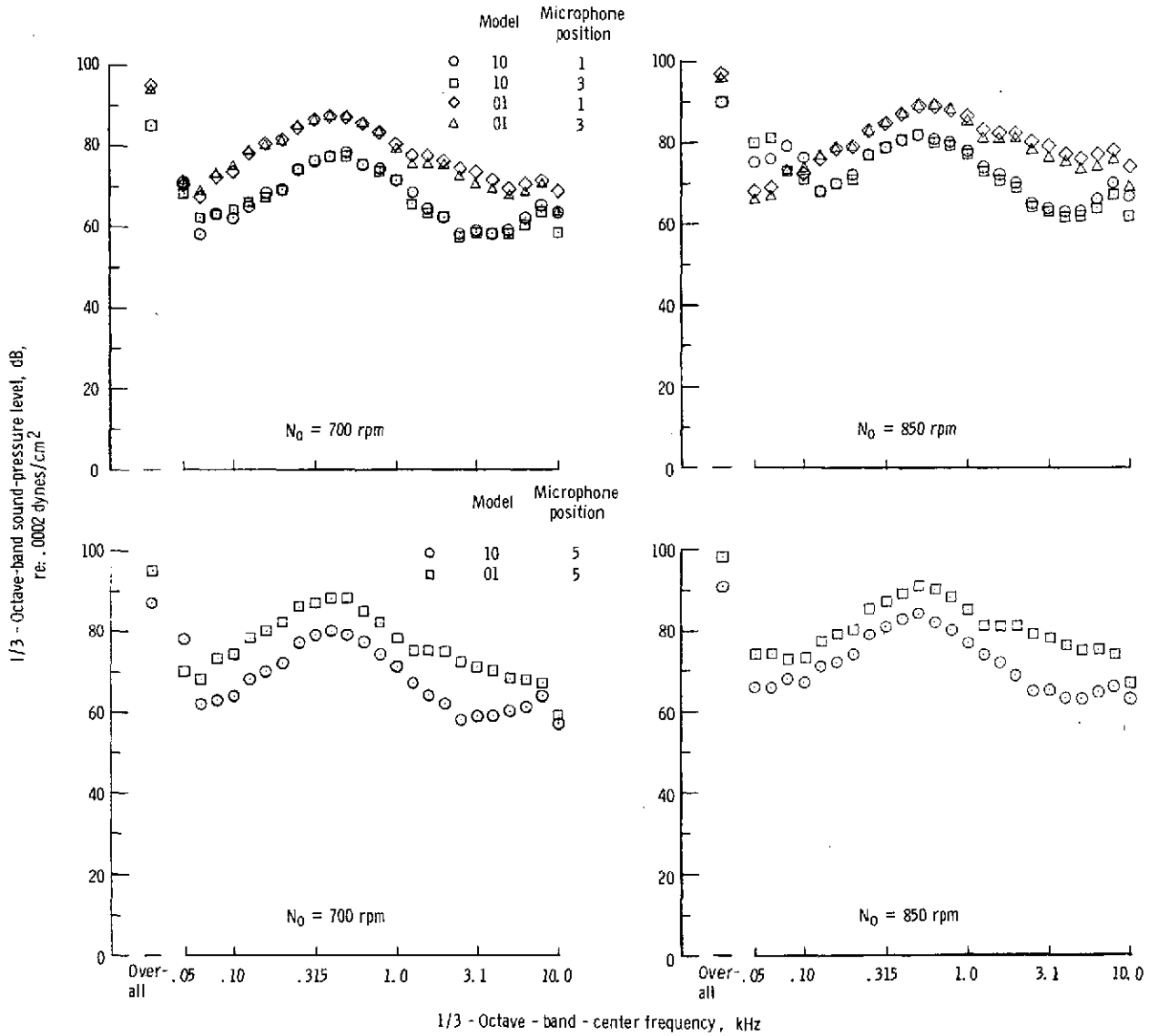

Figure 27.- Comparison of noise of rotors with cylindrical blades (model 01) and airfoil blades (model 11) with V = 0.

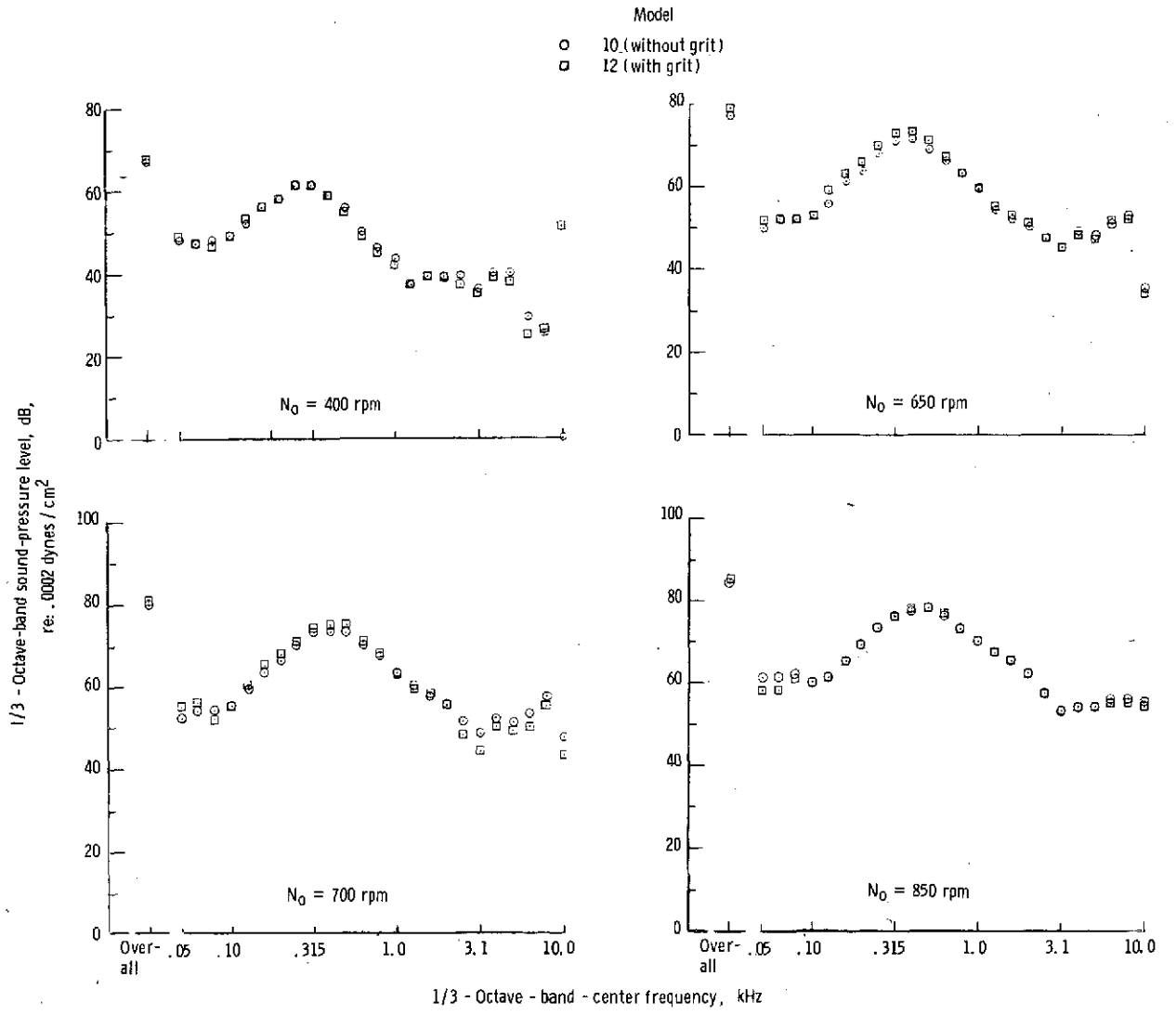

(a) Microphone alined with rotational axis (position 10).

Figure 28.- Effect of No. 14 grit on leading edge of rotor with airfoil blades.

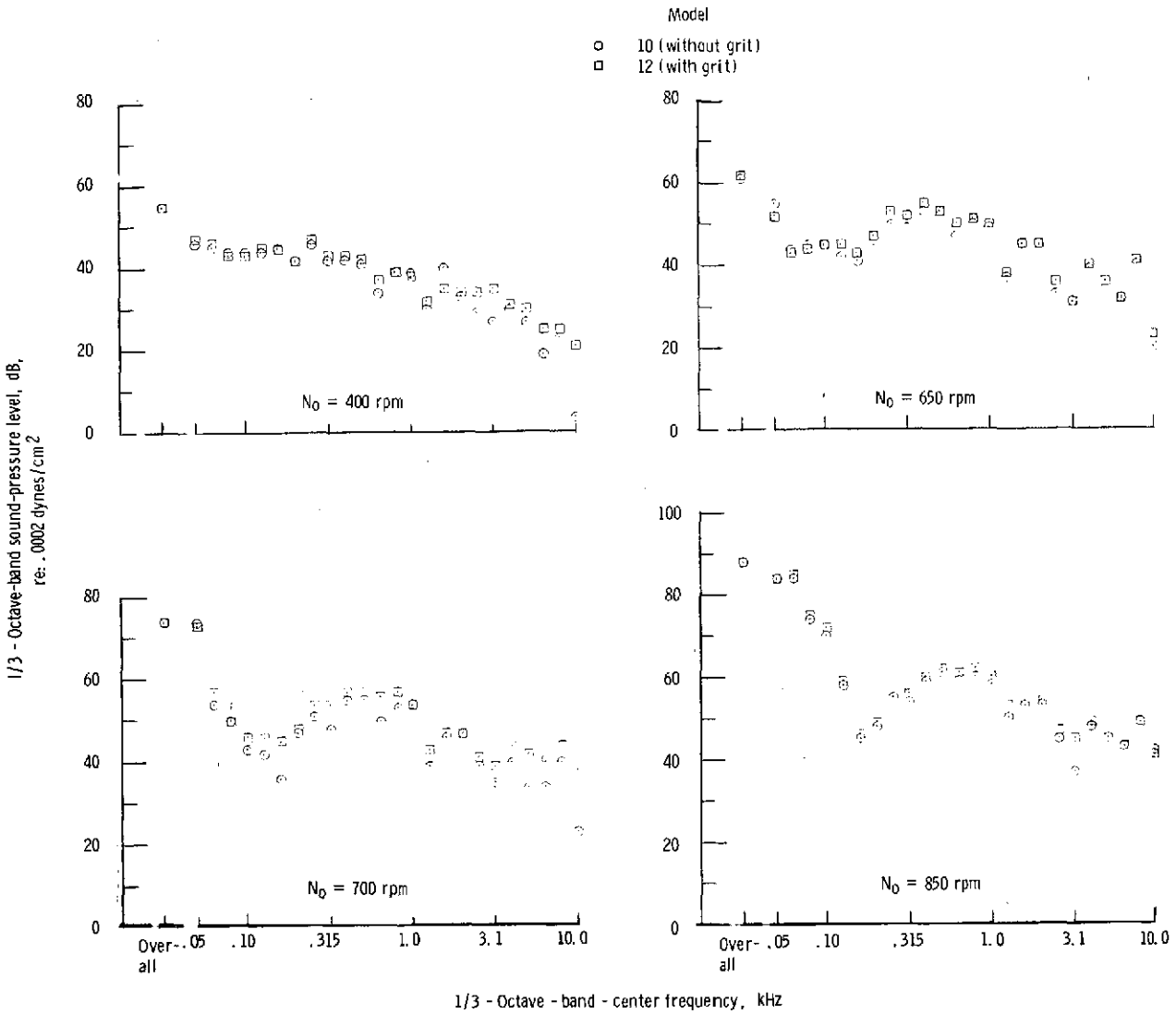

(b) Microphone in plane of rotation (position 15).

Figure 28.- Concluded.

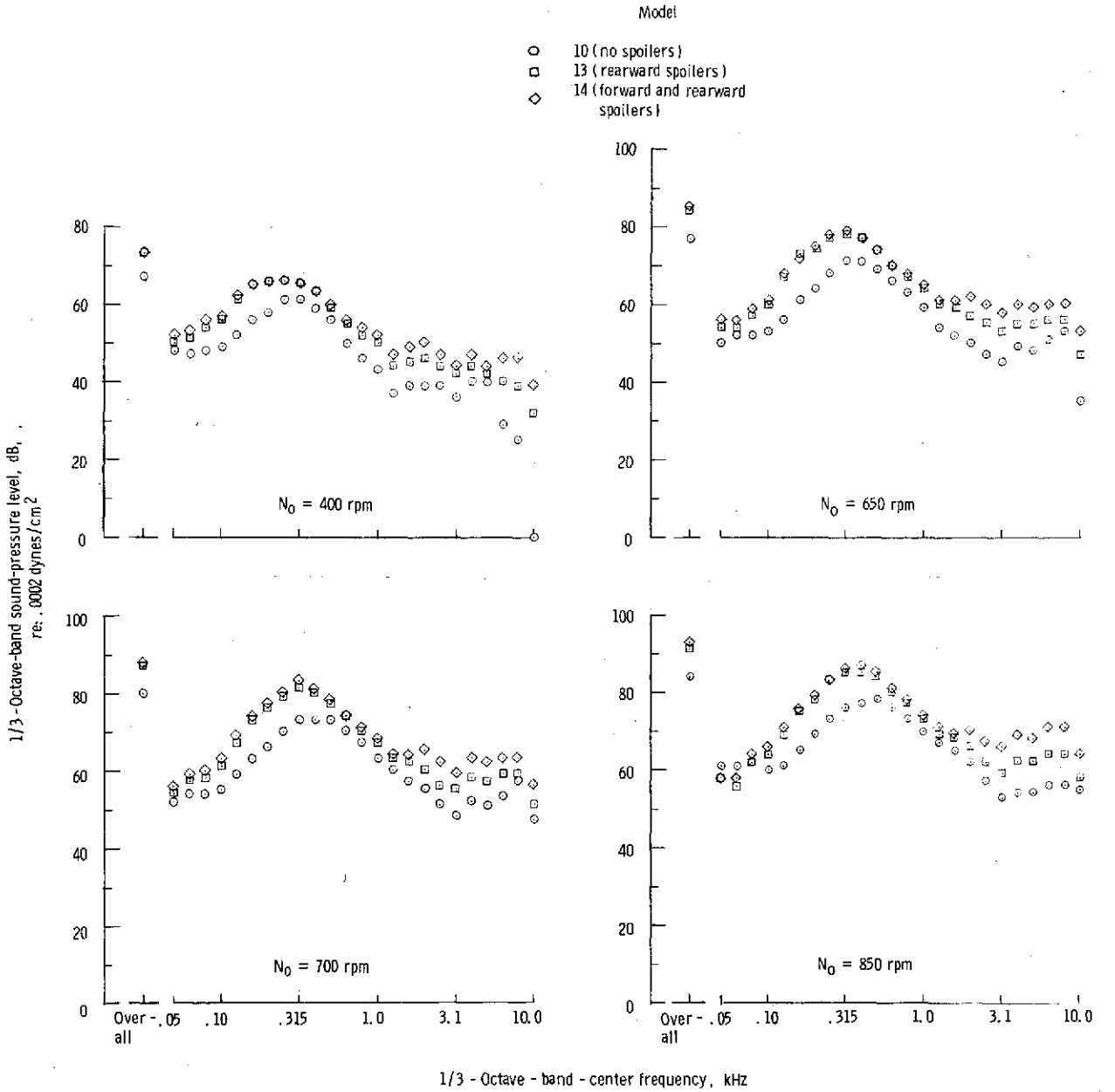

(a) Microphone alined with rotational axis (position 10).

Figure 29.- Effect of adding spoilers to the rotor with airfoil blades. V = 0.

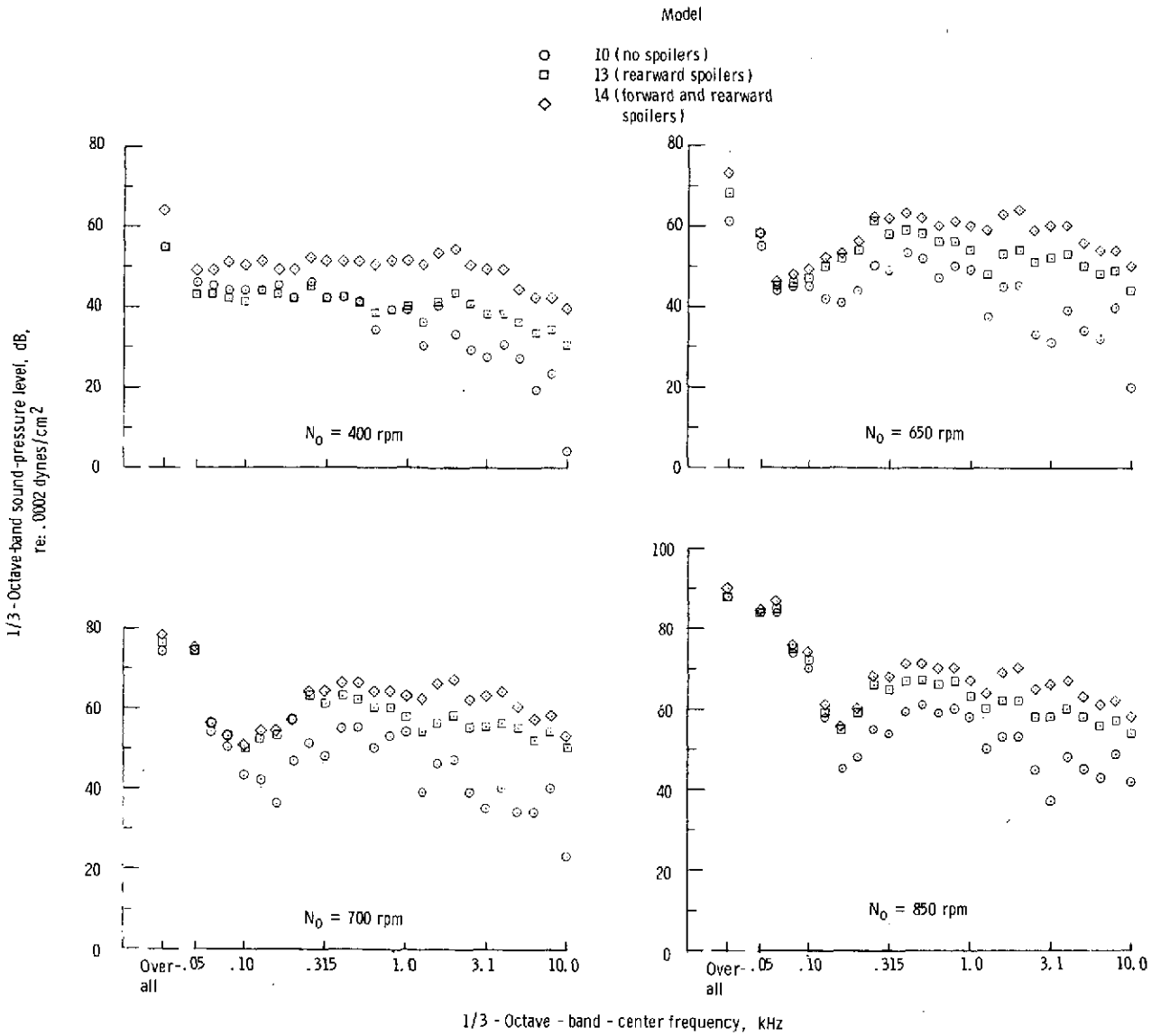

(b) Microphone in plane of rotation (position 15).

Figure 29.- Concluded.

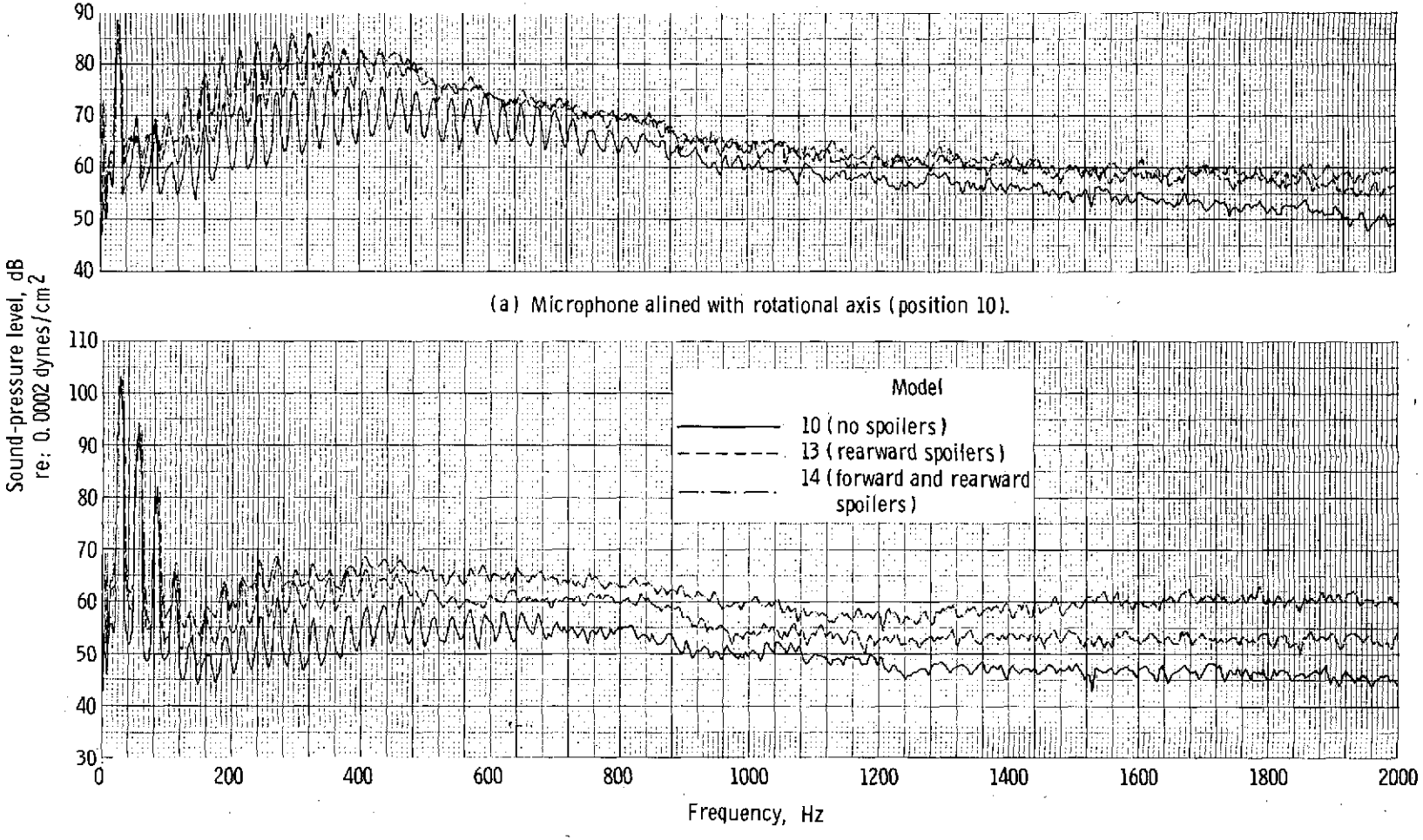

(a) Microphone alined with rotational axis (position 10).

(b) Microphone in plane of rotation (position 15).

Figure 30.- Effect of spoilers. N_0 = 850 rpm; V = 0.

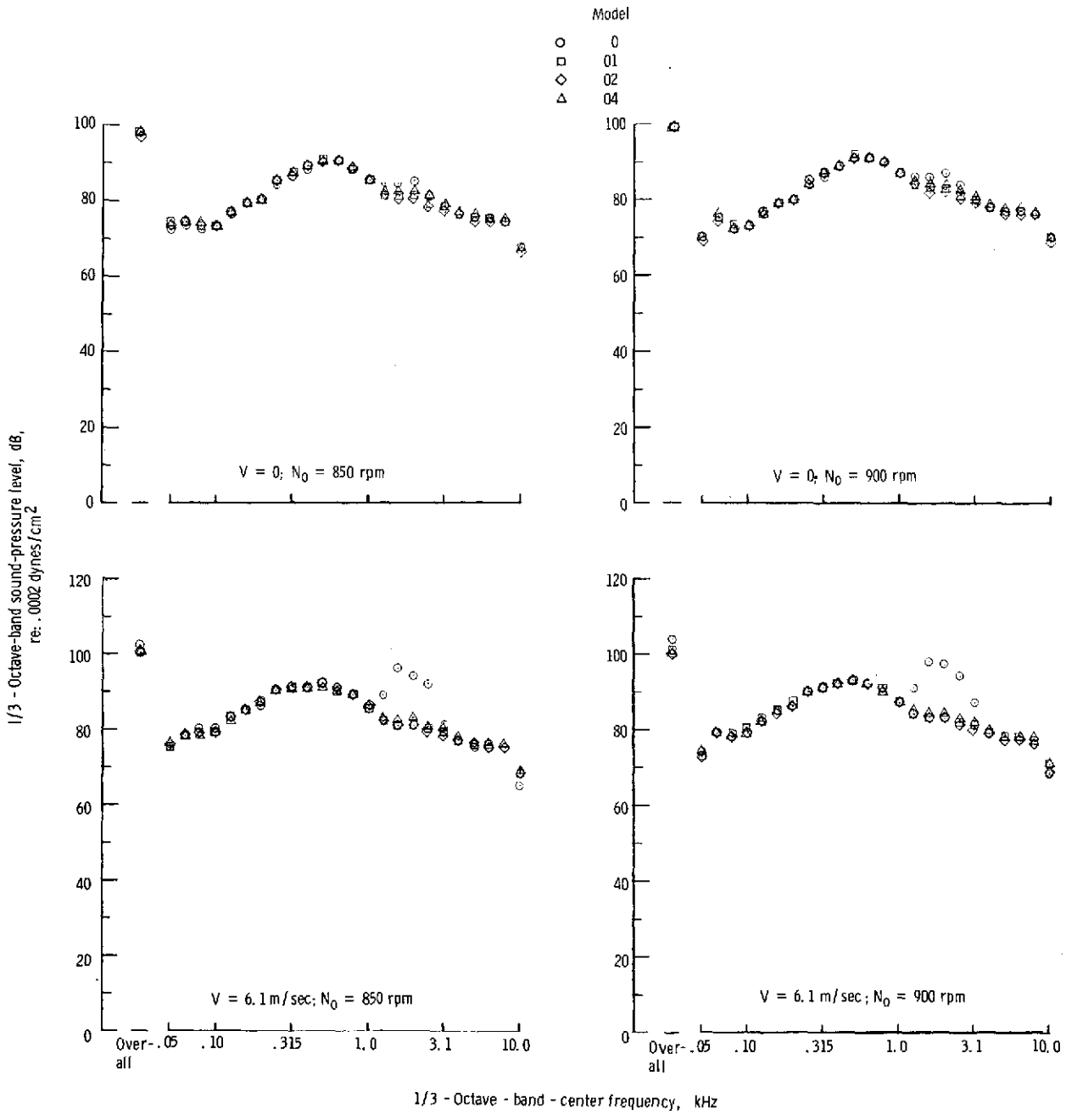

(a) Microphone alined with rotational axis (position 5).

Figure 31.- Effect of tip shape for rotor with cylindrical blades.

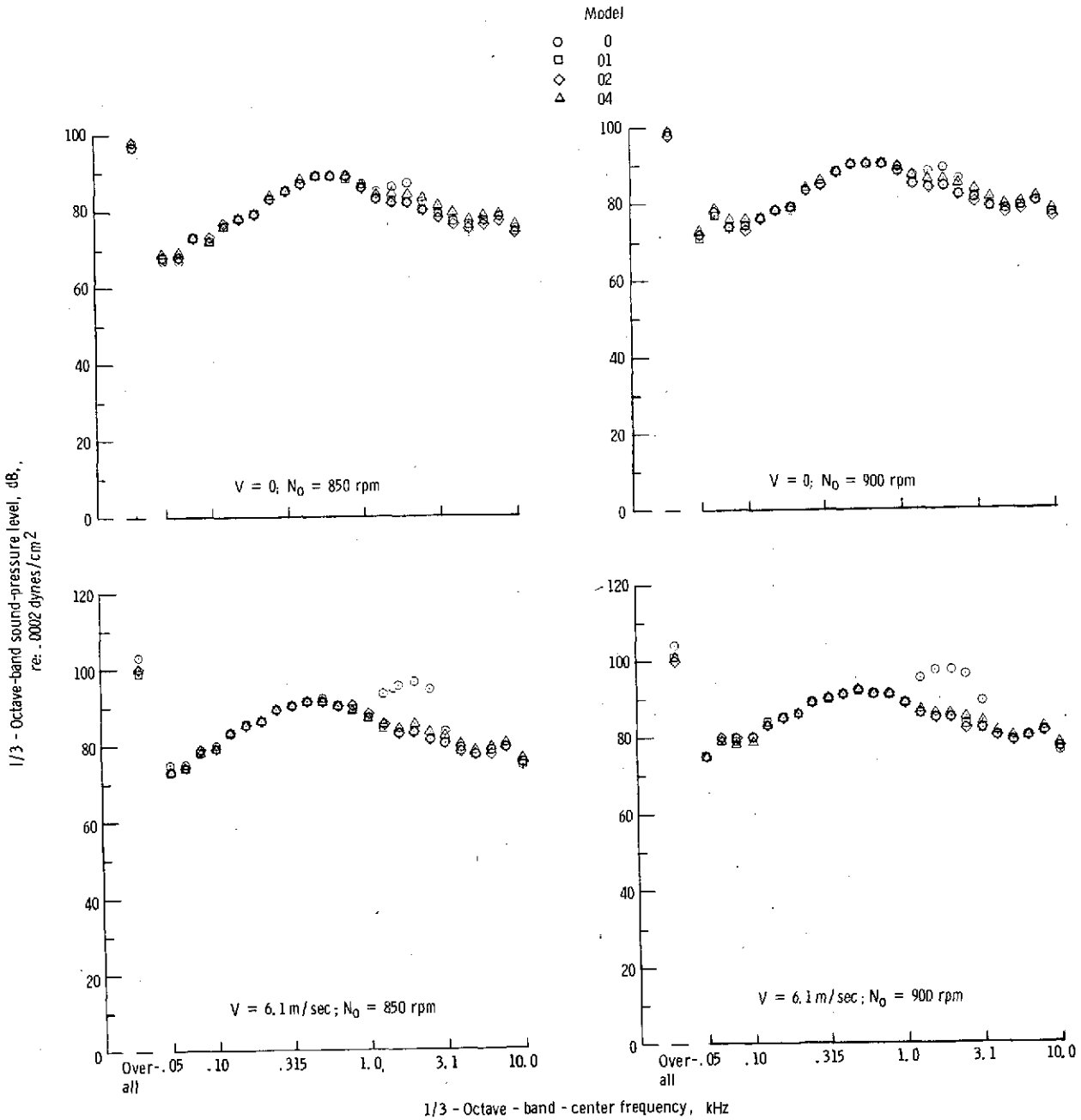

(b) Microphone at 45° to rotational axis (position 3).

Figure 31.- Concluded.

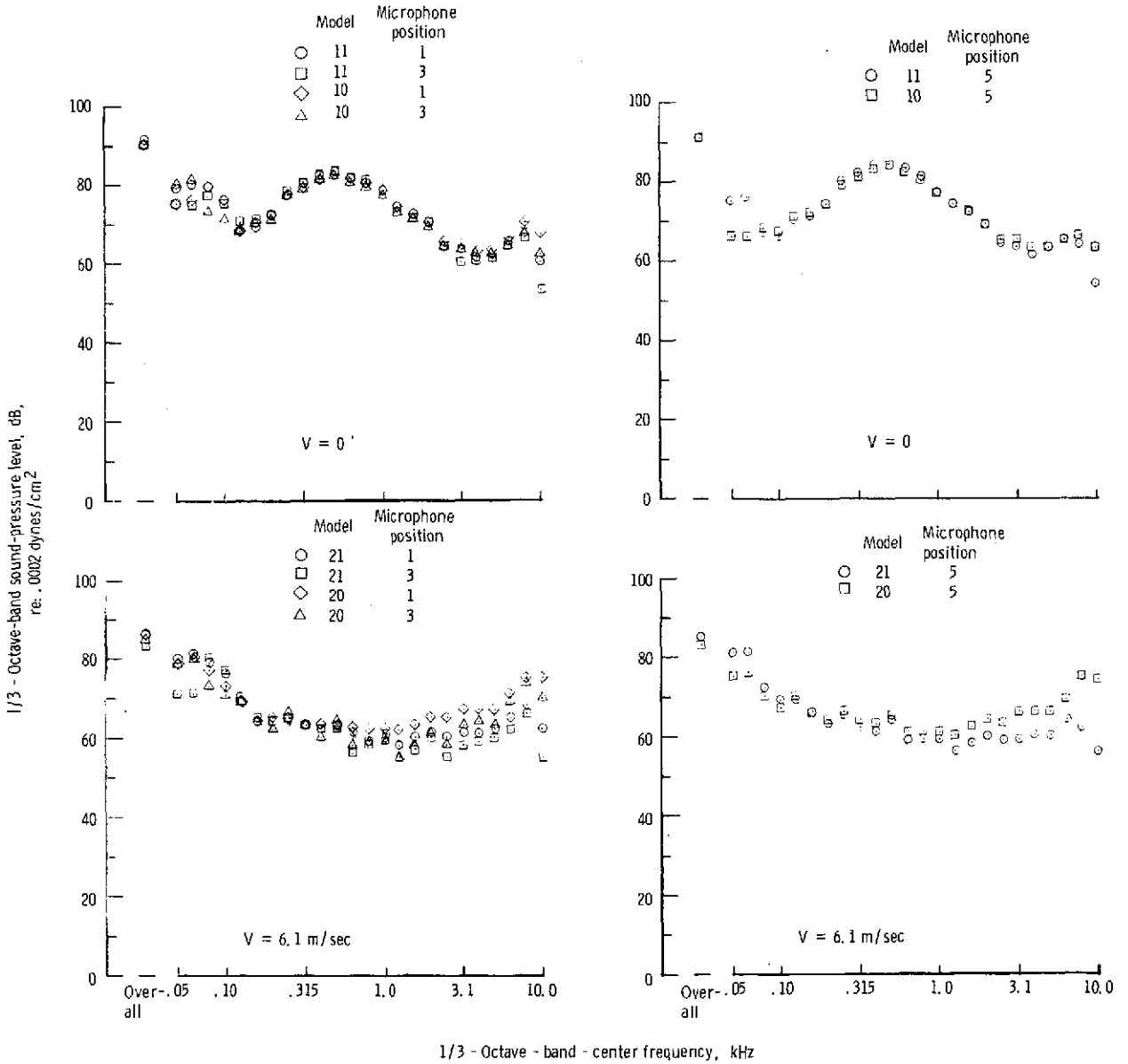

Figure 32.- Effect of tip shape for rotor with airfoil blades. N_0 = 850 rpm.

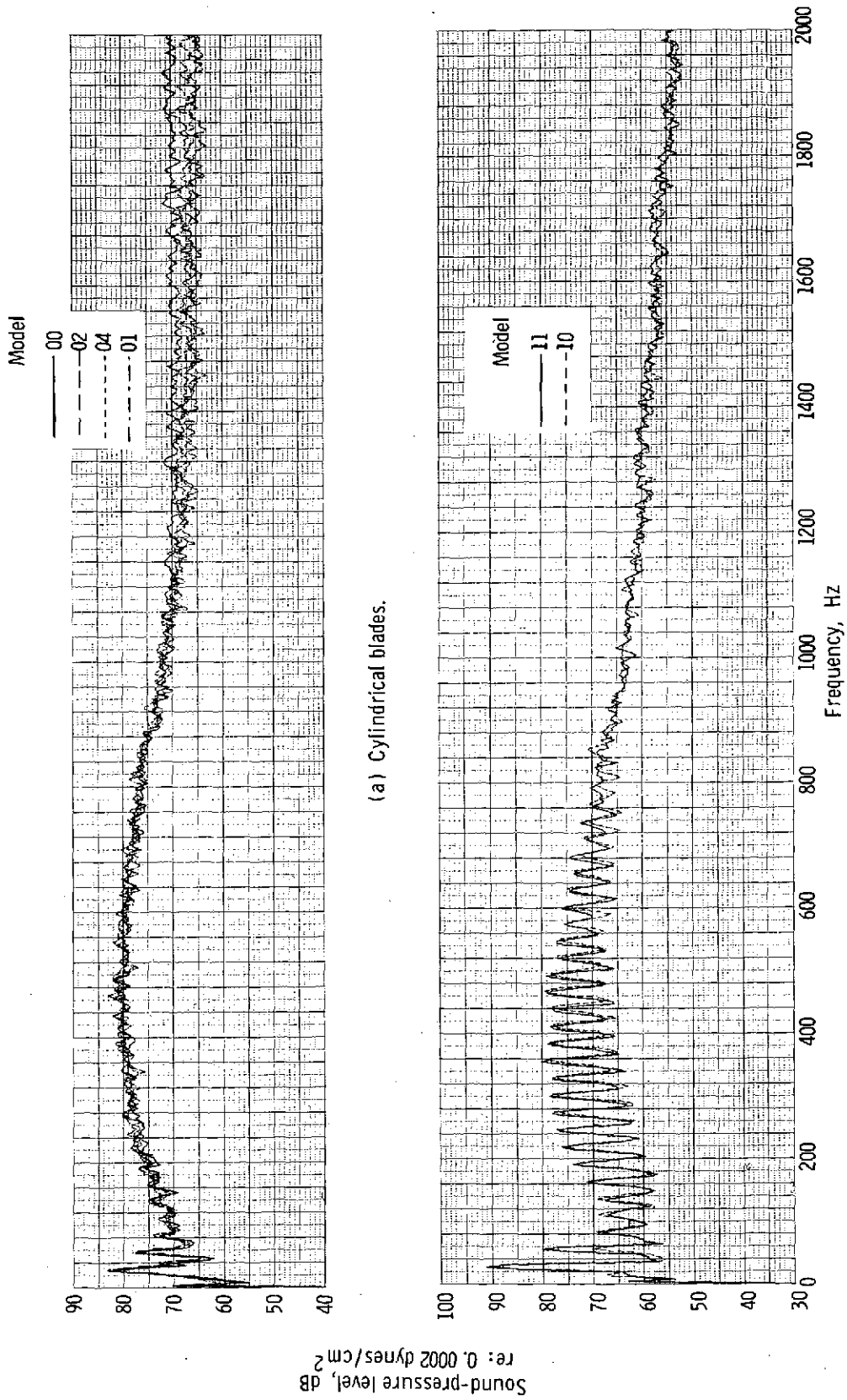

Figure 33.- Effect of blade-tip shape. N_0 = 850 rpm; V = 0. Microphone alined with rotational axis (position 5).